EG&G Idaho, Inc.

FORM EG&G 398
(Rev. 11-79)

INTERIM REPORT

Accession No. _____

Report No. EGG-CAAD-537.

Contract Program or Project Title: Code Assessment and Applications Division

Subject of this Document: TRAC-P1A and TRAC-PD2 Calculations for a 0.10 M Diameter Cold Leg Break and TRAC-PD2 Calculation of a Single Steam Generator Tube Rupture in a Pressurized Water Reactor

Type of Document: Preliminary Assessment Report

Author(s): P. D. Wheatley

NRC Research and Technical Assistance Report

Date of Document: February 1981

Responsible NRC Individual and NRC Office or Division: J. Guttmann, NRC-NRR and F. Odar, NRC-RSR

EG&G Idaho, Inc.
Idaho Falls, Idaho 83415

Prepared for the
U.S. Nuclear Regulatory Commission
Washington, D.C.
Under DOE Contract No. DE-AC07-76ID01570
NRC FIN No. A6047

INTERIM REPORT

ABSTRACT

To investigate the capability of TRAC-P1A and TRAC-PD2 to calculate the phenomena associated with a small break in the cold leg of a pressurized water reactor, calculations were performed for a 0.10 m diameter break with each verison of TRAC. To determine the relative capabilities of each version of TRAC the results of the calculations are compared. The results of each TRAC calculation are compared with results from a RELAP4/MOD7 calculation of a similiar transient. Calculated results are qualitatively compared against LOFT and Semiscale experimental test data.

A TRAC-PD2 calculation, performed to predict the response of the Westinghouse Zion 1 PWR to a 200% offset break in a single steam generator tube, is also reported.

SUMMARY

The Westinghouse Zion I pressurized water reactor (PWR) was modeled using the Transient Reactor Analysis Code (TRAC). Calculations were performed simulating a small cold leg break using the P1A and PD2 versions. A calculation with a single steam generator tube rupture was performed using the PD2 version of the TRAC code.

Results of two TRAC small cold leg break calculations performed with the P1A and PD2 versions were compared to evaluate the capabilities of each version to calculate the behavior during a small break loss-of-coolant accident. These calculations were also qualitatively compared with a RELAP4/MOD7 calculation of the same accident and with the trends of experimental data from LOFT and Semiscale tests which simulated similar transients.

The comparisons indicate that both versions of TRAC were capable of calculating the general system hydraulics and core thermal response for a small cold leg break. TRAC-PD2 was also capable of calculating the general hydraulic response of the rupture of a single steam generator tube.

ACKNOWLEDGEMENTS

The author of this report wishes to thank A. C. Peterson and C. D. Fletcher for providing important advice in the preparation of this report. I would like to express my appreciation to Dawnie Terry, Engineering Assistant, for her outstanding effort and timely contributions. I would also like to thank Joan Mosher for her efficiency and patience in the timely preparation of this report.

CONTENTS

FIGURES

TABLES

1. INTRODUCTION

Two small break calculations and one steam generator tube rupture calculation have been performed with the TRAC computer code which was developed at Los Alamos Scientific Laboratory (LASL). TRAC-P1A[1] and TRAC-PD2[2] were used to analyze a 0.10 m-diameter cold leg break in the Westinghouse Zion I pressurized water reactor (PWR). TRAC-PD2 was also used to analyze the effects of a single steam generator tube rupture in the Westinghouse Zion I PWR. All three calculations used the same basic model so that direct comparisons of the results from different versions of the computer code were possible. These three calculations are part of the ongoing assessment of TRAC being conducted at the Idaho National Engineering Laboratory (INEL).

The Transient Reactor Analysis Code (TRAC) is an advanced best estimate computer code for PWR Loss-of-Coolant Accident (LOCA) analysis. TRAC-P1A and TRAC-PD2 both allow three-dimensional representation of the reactor vessel with two-fluid nonequilibrium hydrodynamic models. All other components are represented one-dimensionally with two-phase nonequilibrium fluid dynamic models. Both versions provide consistent treatment of entire accident sequences including the generation of consistent initial conditions. TRAC-PD2 includes improvements in numerical techniques resulting in improved mass conservation. The vessel heat transfer package in TRAC-PD2 has been refined and allows a more accurate tracking of quench fronts. Description of the code, model nodalization, code options, and initial conditions are found in Section 2.

The two small break calculations were run through blowdown and were concluded after accumulator injection had started and all rods had been reflooded. The steam generator tube rupture calculation was concluded after safety injection flow exceeded flow through the ruptured steam generator tube and primary system mass was increasing. Section 3 gives a detailed discussion of each calculation. Comparisons with a similar

calculation using the RELAP4/MOD7 computer code are also made for the small break calculation. The conclusions and recommendations of this report are contained in Section 4 and References are found in Section 5. A complete input listing is presented for the TRAC analysis in Appendix A.

2. MODEL DESCRIPTION

The calculational model was developed using the Zion I pressurized water reactor as a basis for providing input to the TRAC computer code. The input data came from three sources: the BE/EM study,[3] a PWR model developed by LASL[1] and the Safety Analysis Report for the Zion I pressurized water reactor.[4] The BE/EM study[3] was the primary source of information unless more complete information was available elsewhere. The following sections briefly describe the code versions used, model nodalization, code options, and the initial and boundary conditions for the calculations.

2.1 Code Description

Two releases of the TRAC computer code were used for the reported calculations. TRAC-P1A was used with the updates described in the TRAC Newsletter No. 1.[5] TRAC-PD2 was used without updates. The Configuration Control Numbers for the TRAC-P1A and TRAC-PD2 are H0038858 and H0020858, respectively at the Idaho National Engineering Laboratory.

2.2 Nodalization

The model used for both small break calculations was nearly the same. The model contained 32 components with 175 total cells. A two loop model was chosen due to the anticipated length of the calculations and the resulting computer time. The broken loop, representing one of the four Zion primary coolant loops, modeled the volumes, flow areas and lengths of a single PWR loop. The intact loop was a composite of the remaining three loops. The volumes and flow areas were increased by a factor of three to model the correct loop mass and fluid velocities. Each loop contained 15 components resulting in a total of 31 one dimensional components, including the break. The component configuration along with a view of level 10 in the vessel is shown in Figure 1.

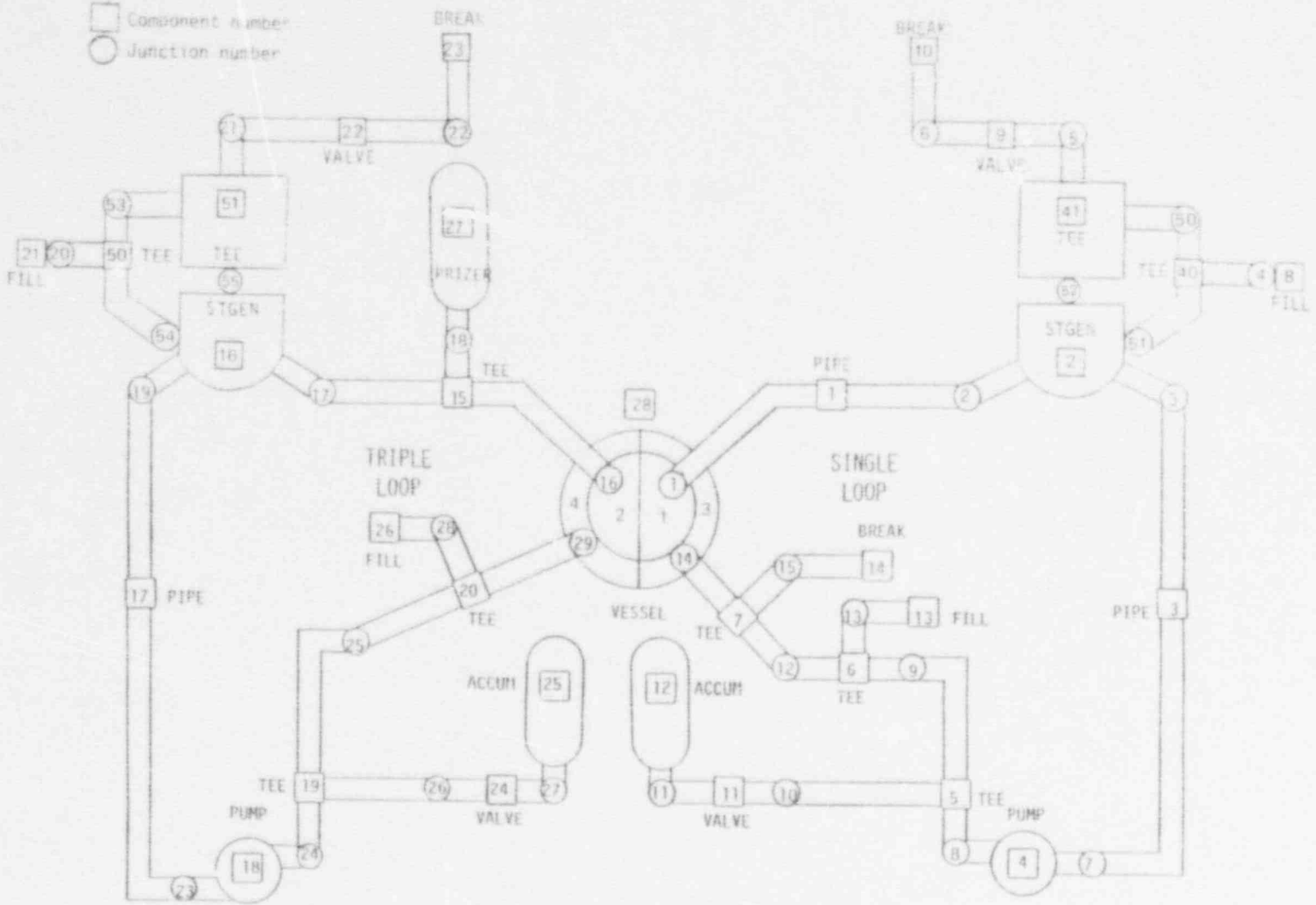

Figure 1. TRAC nodalization of Zion I.

The steam generator secondaries in both the loops were modeled with a recirculation path. This modeling was performed by using the steam generator component in conjunction with two tees as shown in Figure 2. The steam generator component modeled the steam generator up to the normal water level. The upper part of the steam generator was then modeled as a tee with the secondary side representing the recirculation path. The downcomer was also modeled as a tee with the secondary side of the tee accommodating the feedwater fill. The TRAC-P1A model included atomspheric dump valves on the steam generator secondary which were not challenged and were excluded in the TRAC-PD2 model.

The break was modeled using a tee component to simulate a communicative break. The secondary side flow area was 0.0081 m^2 which corresponds to a 0.10 m-diameter break. The noding of the tee secondary side is shown in Figure 3. The first secondary cell was lengthened to 5 m in the TRAC-PD2 calculation to avoid Courant limiting. The lengthening of the secondary cell was believed to have a minimal affect on the calculation since the break flows from the two calculations were nearly the same early in the transient.

The reactor vessel was modeled with 12 axial levels with each level subdivided into two radial rings and two azimuthal zones for a total of 48 mesh cells. Figure 4 shows an axial cross section of the vessel. The downcomer region was modeled by the outer ring between levels 3 and 11.

The lower plenum was noded with three levels. Levels 4 through 8 contained the core permitting the representation of an axial power distribution. In addition to the average rods, two rods were included to model hot rods. The upper plenum was noded with three levels: level 9 below the inlet and outlet nozzles, level 10 which spanned the outlet nozzle flow region, and level 11 above the nozzles and below the upper head. Level 12 represented the upper head region of the vessel.

The small break model was modified by the addition of a tee and a valve to simulate a steam generator tube rupture. Figure 5 shows the

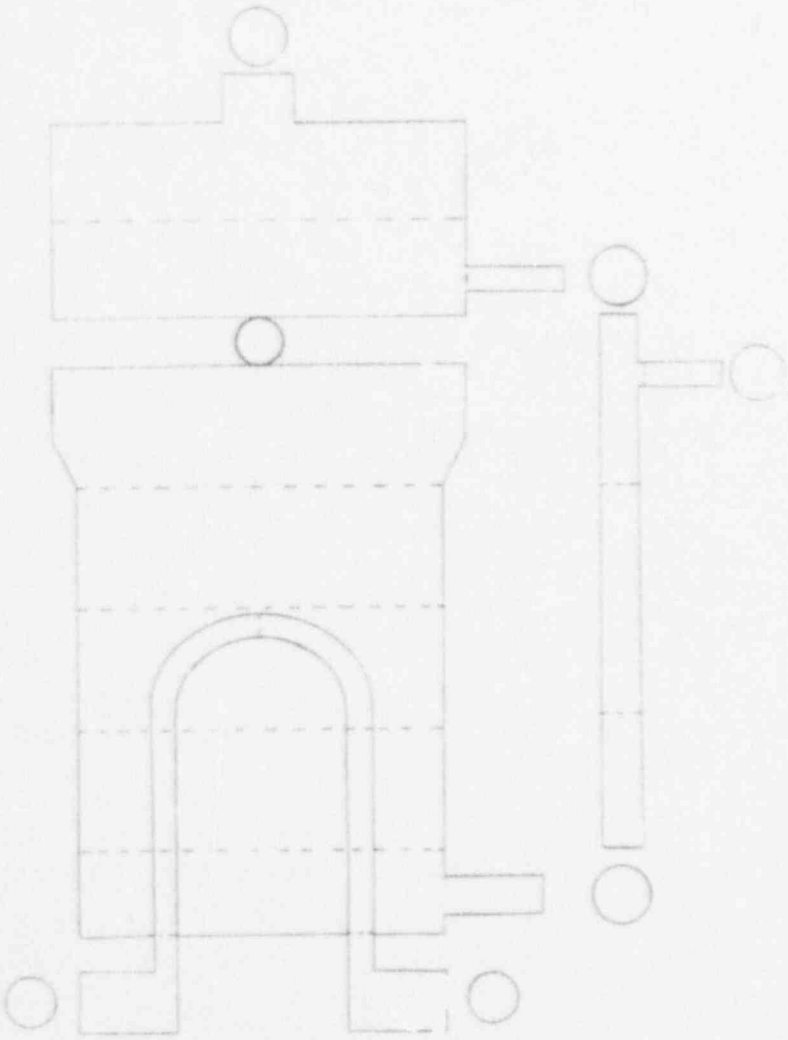

Figure 2. Steam generator nodalization.

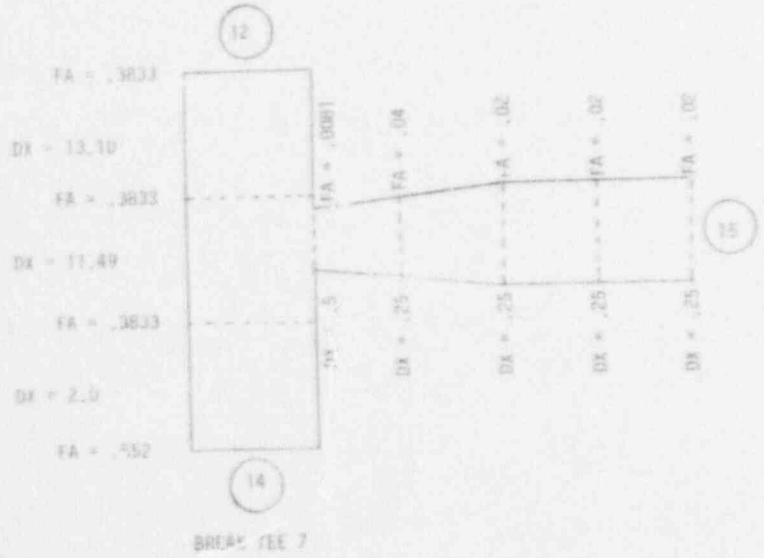

Figure 3. Break nodalization.

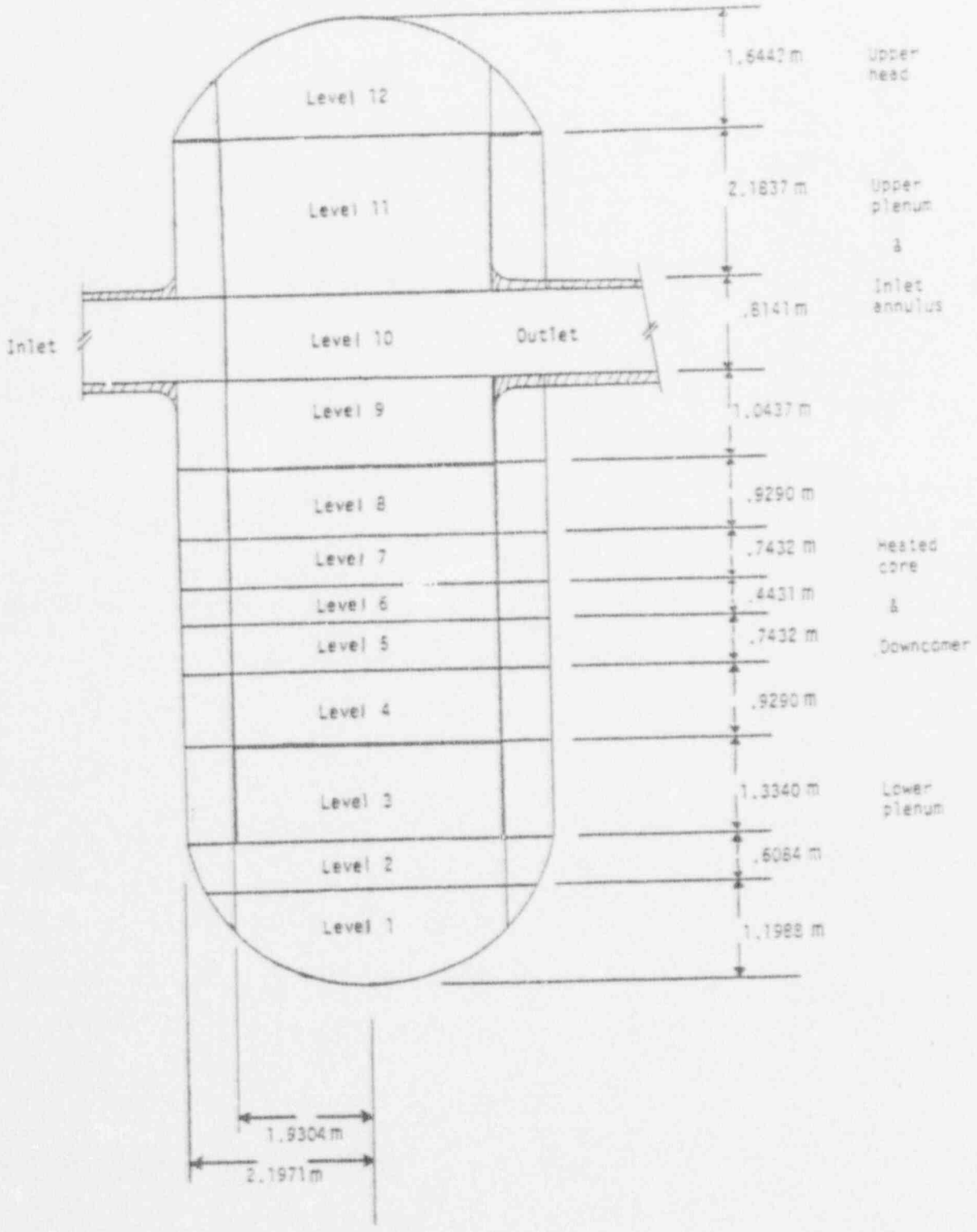

Figure 4. Zion I vessel noding for TRAC.

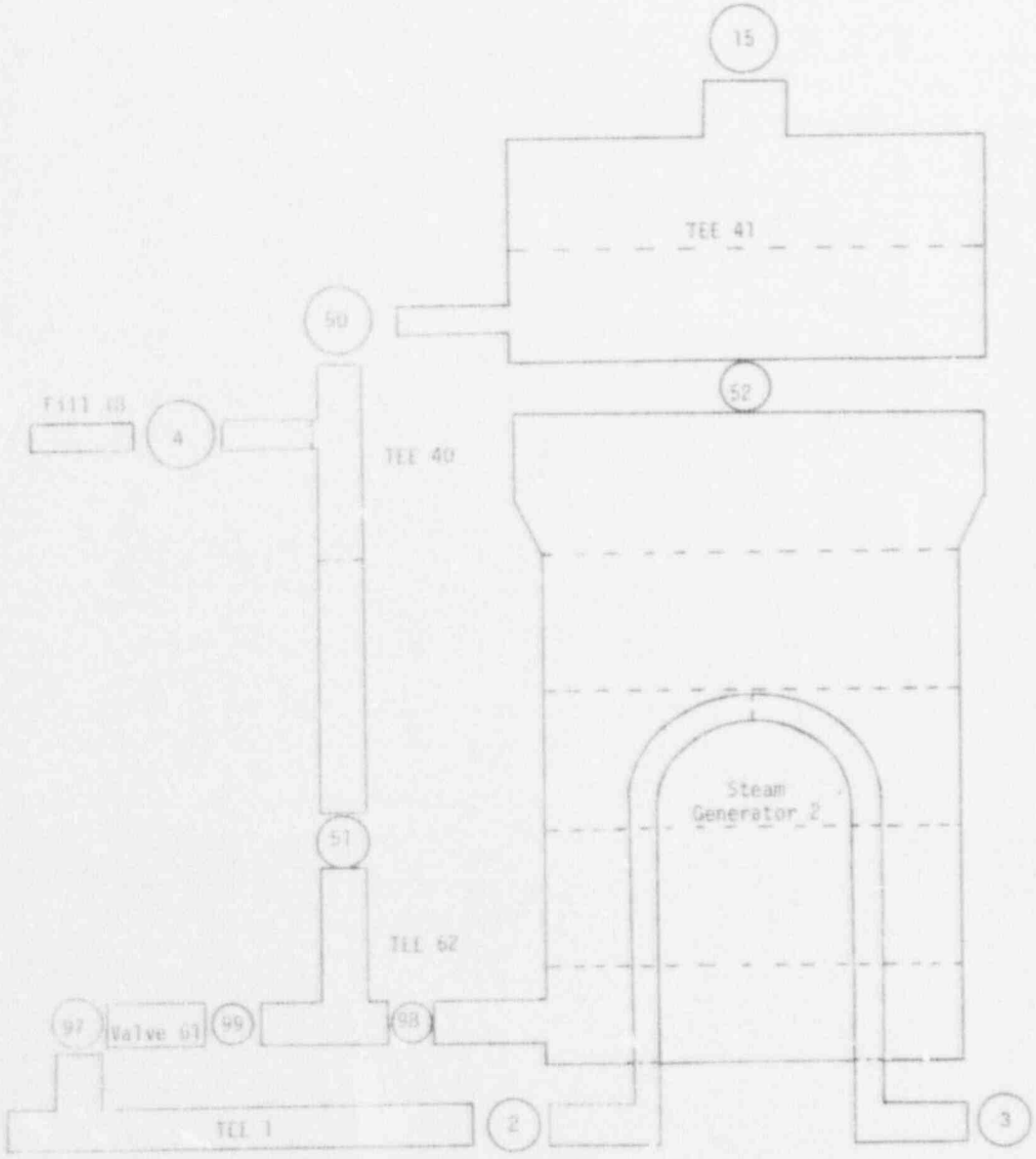

Figure 5. Steam generator configuration for steam generator tube rupture.

component configuration for the steam generator tube rupture. A direct method of modeling a steam generator tube rupture was not available within TRAC. Flow from the hot leg (TEE 1) was routed through a valve to the first cell of the steam generator secondary. This configuration represents a tube rupture at the tubesheet. Complete code input listings of the three calculations are presented in Appendix A.

2.3 Code Options

TRAC-P1A and TRAC-PD2 require a minimum of input selection. A major choice is the friction factor correlation to be used in components other than the vessel. Based on the TRAC Developmental Assessment Report,[6] the annular flow correlation (NFF=4) was selected for all components.

The option using the input of a fuel rod gap conductance was selected. A value of 6600 $w/m^2/K$ was chosen based on previous calculations.[7]

The partially implicit numerical hydrodynamics option (IHYDRO=0) was used throughout the loop piping except for the piping adjacent to the break and pressurizer where the fully implicit option (IHYDRO=1) was used.

2.4 Initial and Boundary Conditions

A TRAC steady state calculation was used to determine the initial system conditions for the transients. The calculation was run until it met the specified convergence criterion of 1.0×10^{-3}. The initial system conditions are shown in Table 1. The same TRAC-PD2 calculation of steady state was used for both the small break and steam generator tube rupture calculations. The new ANS decay heat rate was used after reactor scram. Safety injection (SI) and charging flows were lumped into a single fill component. Figure 6 shows the injection rate of two HPIS, LPIS and charging pumps as a function of pressure. It was discovered near the end of the two calculations that the charging and SI flow shown in Figure 6 were in error. The flow rates should have been larger by a factor of 4.

TABLE 1. INITIAL CONDITIONS FOR ZION I TRAC CALCULATIONS

Parameter	TRAC-P1A	TRAC-PD2
Core power (MW_t)	3228	3228
Cold leg fluid temperature (K)	550.4	550.5
Hot leg fluid temperature (K)	583.5	583.1
Pressurizer pressure (MPa)	15.65	15.65
Pressurizer liquid volume (m^3)	30.01	30.01
Core mass flow rate (kg/s)	17263	18243
Steam generator secondary pressure (MPa)	4.686	4.696
Accumulator pressure (MPa)	4.155	4.159
Accumulator liquid volume (m^3)	26.63	26.70
Accumulator temperature (K)	325.0	325.0
Average rod peak power rating (kw/m)	26.39	27.31

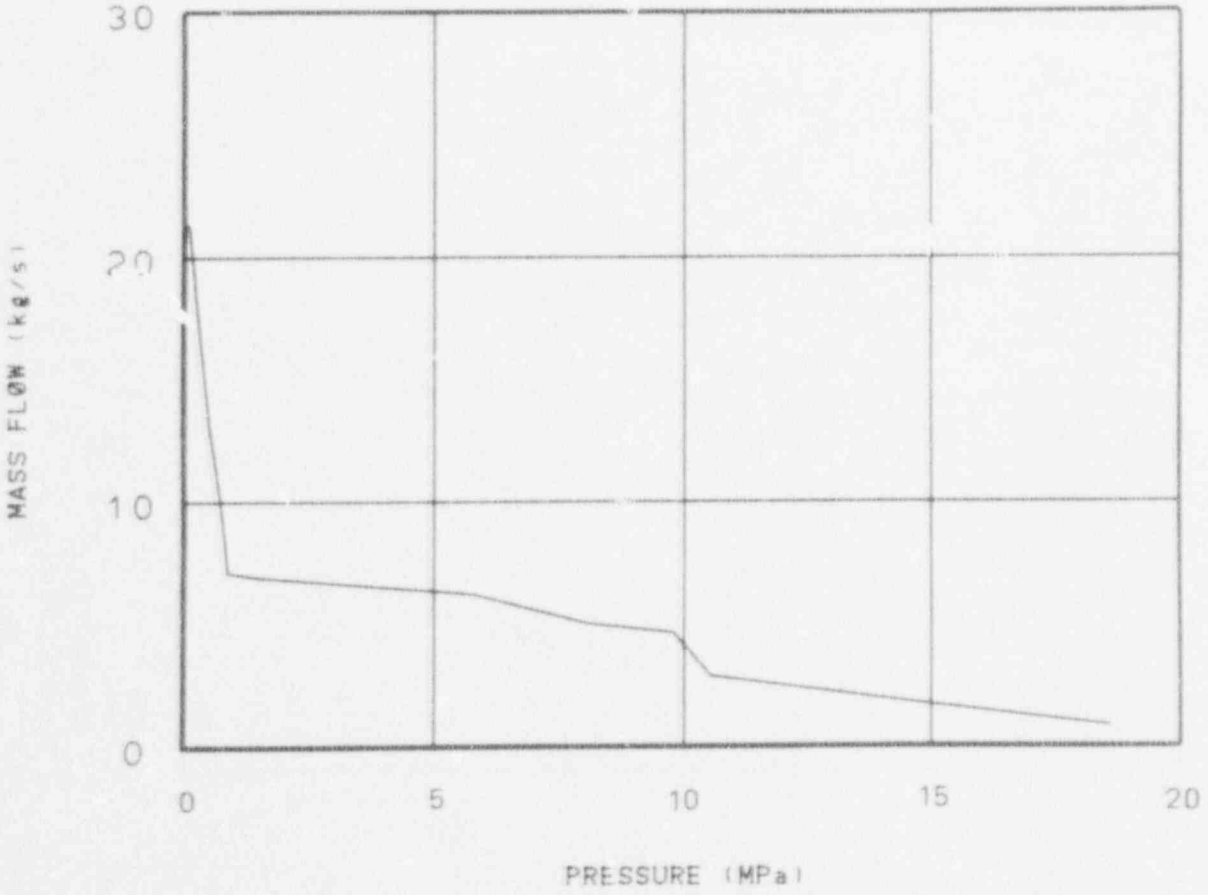

Figure 6. Safety injection and charging flow.

The reduced SI flow decreased the total mass injected into the primary system for the PD2 and P1A calculations. Increasing the SI mass flow by 4 would not have significantly changed the depressurization rate for either calculation. The additional mass in the system for the TRAC-P1A calculation may have maintained a core liquid level and reduced the cladding heat up. The TRAC-PD2 core thermal response would have remained the same since the core was covered throughout the transient. The safety injection and charging flows were corrected for the steam generator tube rupture calculation. Auxiliary feedwater flow was modeled from two motor-driven pumps and one turbine-driven pump. The total flow rate was 28.2 kg/s into the single steam generator and 84.6 kg/s into the triple steam generator at a temperature of 308 K.

3. RESULTS

Calculations using TRAC-P1A and TRAC-PD2 were performed using a CDC 176 computer to simulate a 0.10 m-diameter cold leg break in the Westinghouse Zion I PWR. The TRAC-P1A calculation was concluded 860 s after the rupture requiring 40 hours of CPU time. The TRAC-PD2 calculation required 14 hours of CPU time and was concluded at 673 s into the transient. Both calculations were terminated after initiation of accumulator flow and reflooding of the core had occurred. A calculation using TRAC-PD2 was performed using a CDC 176 computer to simulate a steam generator tube rupture in the Westinghouse Zion PWR. This calculation was run for 600 s using 4.5 hours of CPU time and was terminated when safety injection flow exceeded leakage into the steam generator secondary. Timing of major events for all three calculations is shown in Table 2.

3.1 0.10 m-diameter Cold Leg Break Using TRAC-P1A

The simulated 0.10 m-diameter pipe break occurred at 0.0 s. The system pressure decreased to 12.82 MPa at 9.0 s which resulted in a reactor scram and a primary coolant pump trip after a 3.4 s delay. The steam outlet valves on each steam generator were closed at this time and the feedwater flow ramped off over the next 14 s. Auxiliary feedwater flow was initiated 1 s after termination of main feedwater flow.

Upper plenum pressure, shown in Figure 7, decreased to approximately 6.8 MPa at 50 s which corresponded to the hot leg saturation pressure. The system pressure remained nearly constant until 250 s when the break flow changed from a low quality mixture to predominately steam. The increased volumetric flow rate resulted in an increase in the rate of system depressurization. At 380 s the steam generator secondary pressure equaled the primary system pressure and the primary system depressurization rate decreased due to primary system and steam generator secondary temperatures being nearly equal. The system pressure continued decreasing until 770 s when accumulator fluid quenched the fuel rods. The steam generated from the quenching of the fuel rods increased the system pressure slightly.

TABLE 2. MAJOR EVENT SEQUENCE

Event	Times (s) TRAC-P1A Small Break	TRAC-PD2 Small Break	TRAC-PD2 Steam Generator Tube Rupture
Time of rupture	0.0	0.0	0.0
Reactor scram	12.24	14.36	100.0
Pump trip	12.24	14.36	100.0
Initiation of SI flow	15.11	17.38	105.0
Termination of feedwater	27.24	29.34	120.0
Start of auxiliary feedwater	28.24	30.34	124.0
Broken loop seal swept out	270.0	290.0	--
Termination of auxiliary feedwater	400.0	--	426.0
Initiation of accumulator flow	630.0	462.0	--
Core quenched	775.0	[a]	[a]

a. No core uncovery or rod heat up was calculated.

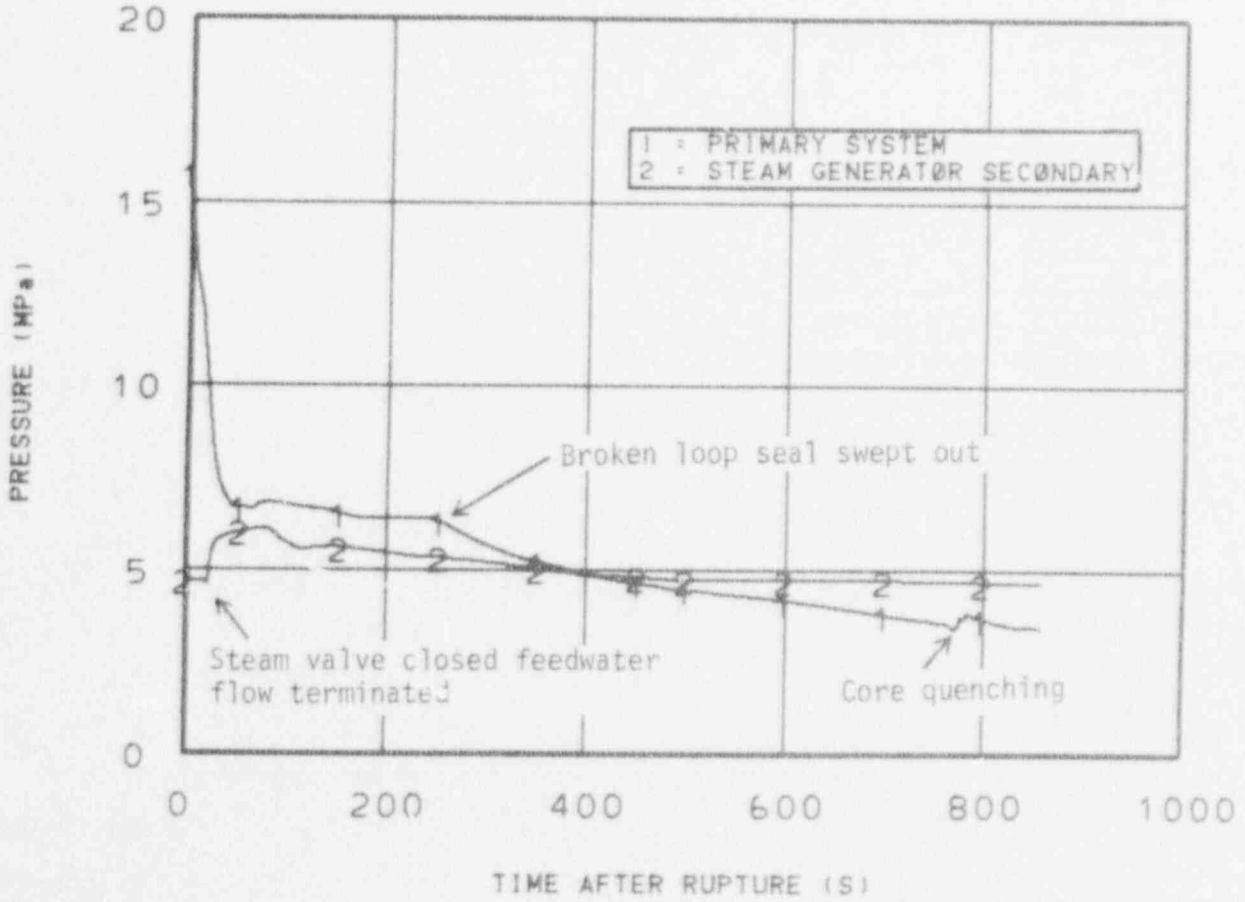

Figure 7. Upper plenum and steam generator secondary pressure (TRAC-P1A).

The steam generator secondary pressure, also shown in Figure 7, increased at 20 s after the steam outlet valve was closed and main feedwater flow decreased. The steam generator secondary began depressurizing after 80 s due to the mixing of subcooled auxiliary feedwater with the steam generator secondary fluid. The secondary side mass inventory increased approximately 4 times faster than the auxiliary feed mass flow rate due to mass gained through numerical errors. The increase in secondary mass reduced the effect of the auxiliary feedwater and resulted in earlier termination of the auxiliary feed flow due to secondary water level recovery. The auxiliary feedwater mixed with the mass gained from numerical errors, which was at the steam generator secondary temperature, resulting in a higher overall secondary temperature. This secondary behavior resulted in a decreased primary depressurization rate and an increase in time to accumulator initiation.

The break mass flow rate, shown in Figure 8, was approximately 900 kg/s initially. The break mass flow rate decreased to 565 kg/s as the system pressure decreased to the hot leg saturation pressure of 6.8 MPa. A sharp drop in break flow occurred at 250 s when the loop seal in the broken loop was swept out. Clearing the broken loop seal permitted vapor flow from the upper plenum which resulted in a high void mixture at the break and decreased the break mixture density. The reduced mixture density at the break resulted in a reduction in the mass flow rate as shown in Figure 8. The instabilities in break flow, starting at 330 s, were a result of renoding the secondary side of the break tee. The renoding was performed to reduce the severely restrictive Courant limit imposed by the code. The instabilities were not fed back into the system and appeared to have little effect on the remainder of the calculation.

Primary coolant flow decreased after the reactor coolant pumps were tripped at 12.24 s. Figure 9 shows the flow coastdown and a flow reversal in the broken cold leg between the vessel and break. Fluid from the downcomer flowed toward the break until 270 s when the loop seal was swept out. During the remainder of the calculation flow was into the vessel due to steam flow from the upper plenum through the loop.

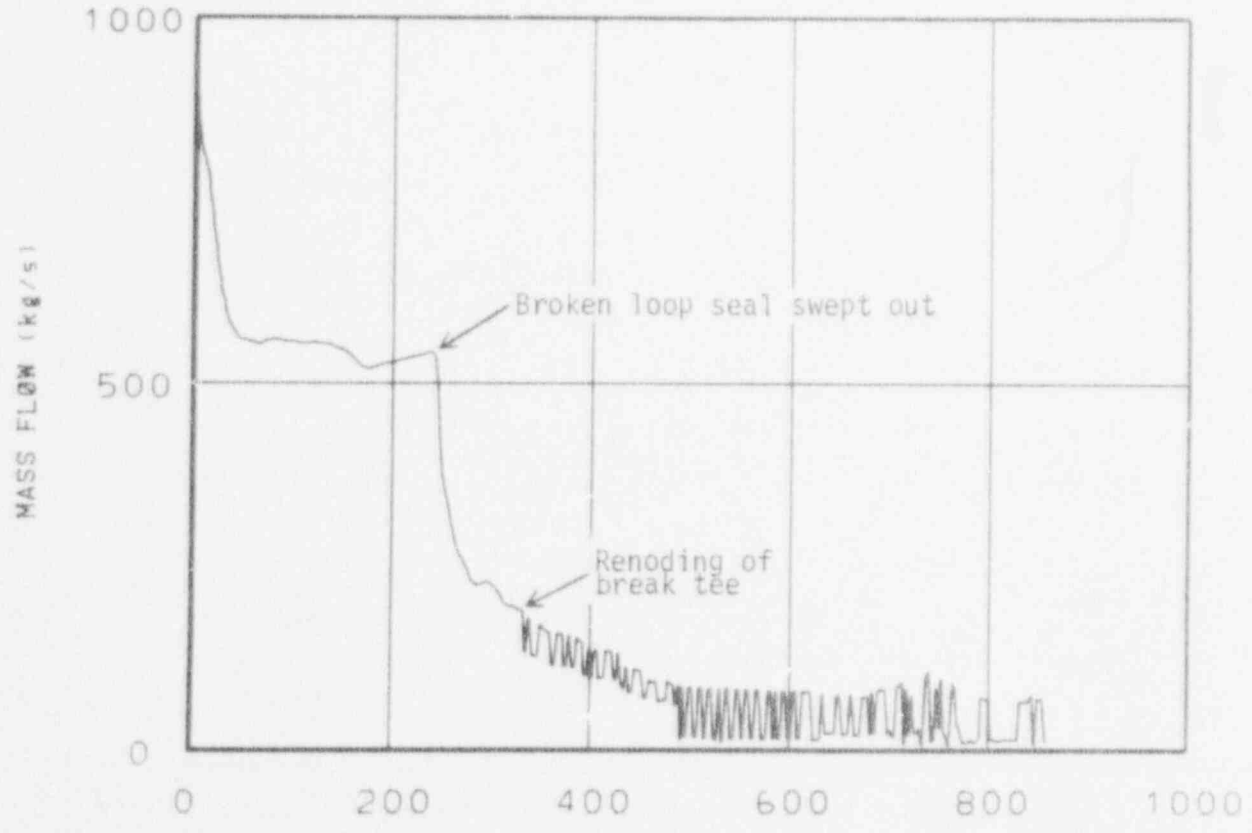

Figure 8. Break mass flow rate (TRAC-P1A).

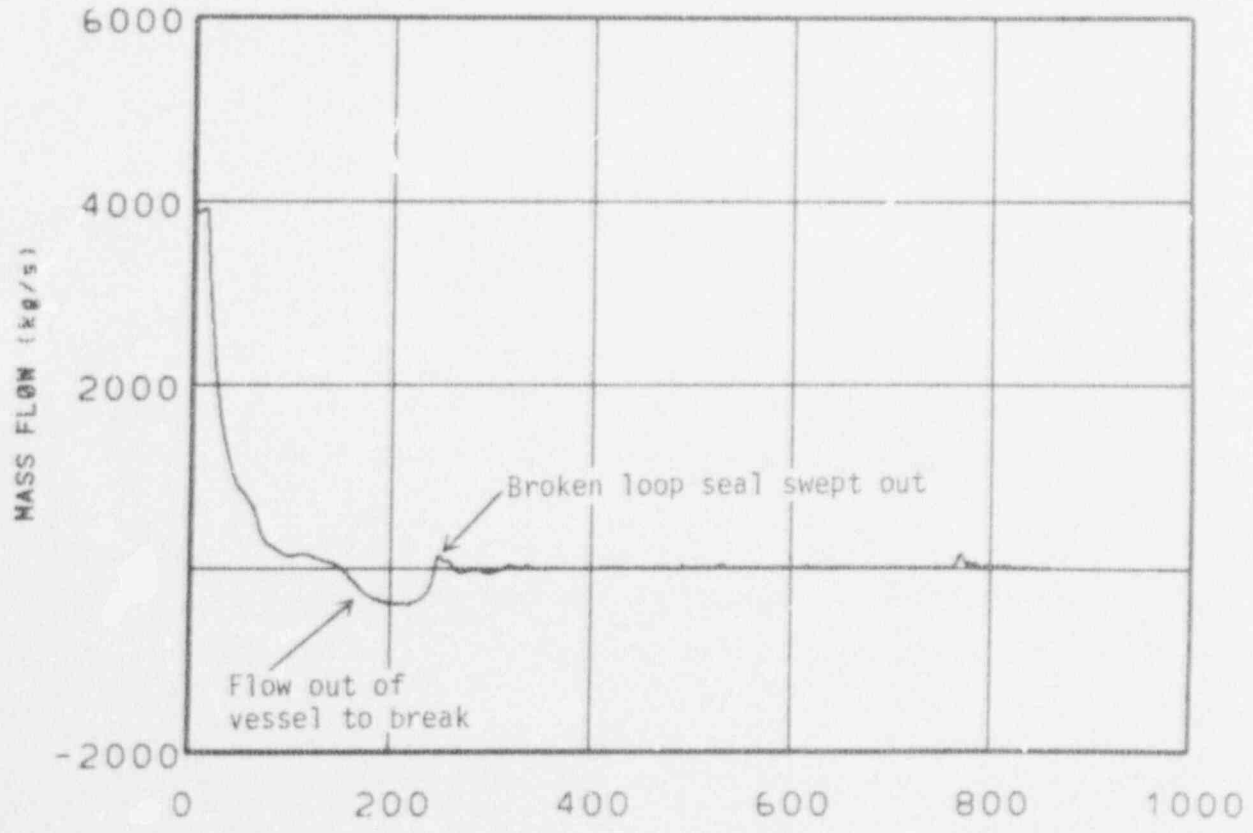

Figure 9. Broken cold leg mass flow rates (TRAC-P1A).

The intact loop cold leg behaved differently due to the loop seal remaining liquid filled and thus blocking the loop flow path. Flow from the loop seal to the vessel was near zero as shown in Figure 10. The intact loop cold leg mixture velocity, shown in Figure 11, was toward the loop seal from 490 s until 660 s. The intact cold leg was being filled with safety injection fluid at 490 s. Figure 12 shows the void fraction in the accumulator injection tee and the safety injection tee of the intact cold leg. When the intact cold leg flow reversed at 490 s, fluid in the tees flowed into the pump and loop seal. Fluid filled each of the computational cells in the intact cold leg from the pump toward the vessel. Each of the computational cells nearly filled before the downstream cell started to fill. This phenomena is not physical as, prototypically, the liquid would tend to form a layer in the pipe and flow toward the vessel. At 630 s, when the accumulator flow was initiated the initial flow was limited due to the intact cold leg being full of liquid. Fluid flowed out of the intact cold leg at 770 s and into the vessel condensing vapor, and allowing an increase in the flow from the cold leg. The void fraction in the intact cold leg increased as fluid drained into the vessel as the vapor in the vessel was condensed. The vessel and core refilled quickly, as shown in Figure 13. Figure 12 shows the void fraction in the intact cold leg decreasing as accumulator fluid once more filled the intact cold leg.

The rod cladding temperature history is shown in Figure 14. Cladding temperatures dropped from near 600 K to the system saturation temperature upon reactor scram at 12.24 s. The rod cladding temperature remained near the fluid saturation temperature being cooled by a two phase mixture in the core. At 575 s the uppermost level of the core dried out and the cladding temperature began increasing. As a result of dry out the clad temperatures in level 4 increased at 615 s followed by the temperature in levels 3 and 2 at 680 s. The lower level of the core experienced no dryout or clad temperature increase. All levels of the core were quenched upon accumulator injection at about 770 s. The peak cladding temperature obtained during the transient was 780 K in level 4 during the dryout.

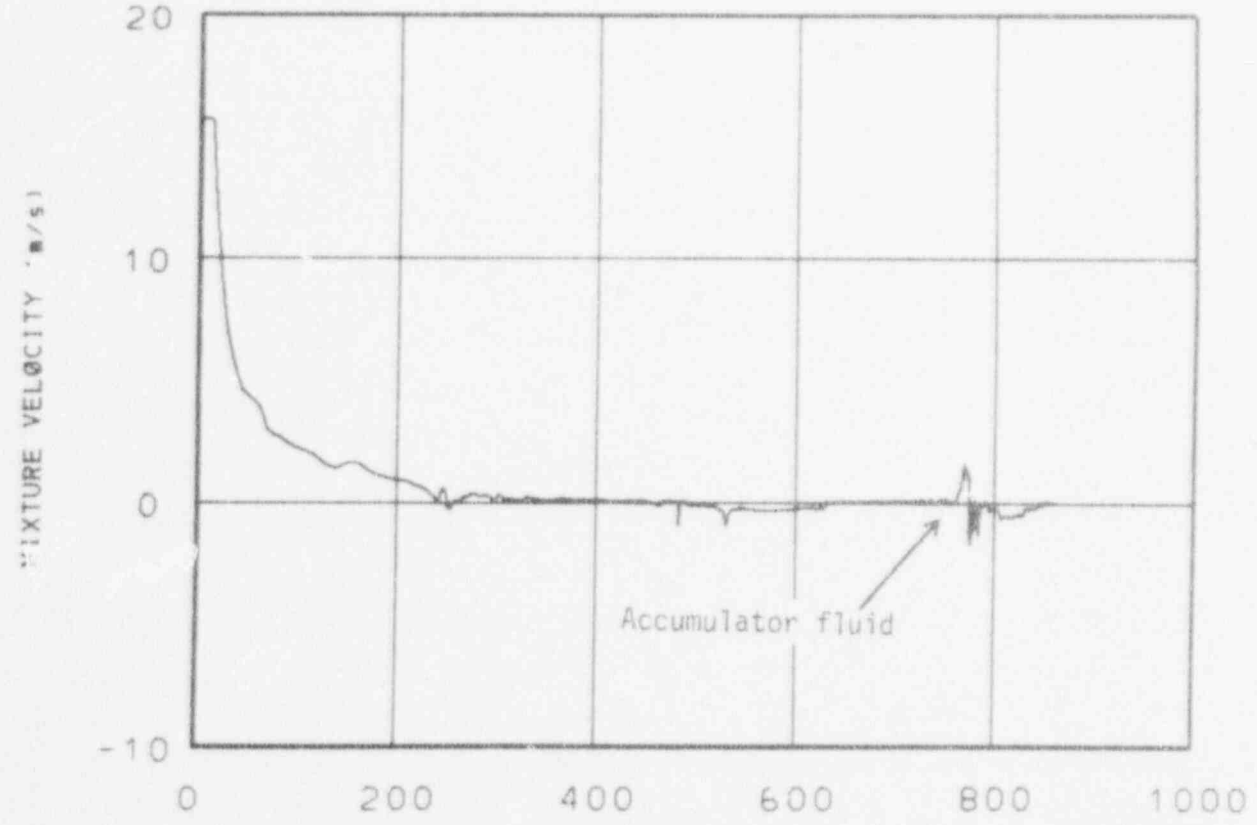

Figure 10. Mixture velocity intact cold leg (TRAC-P1A).

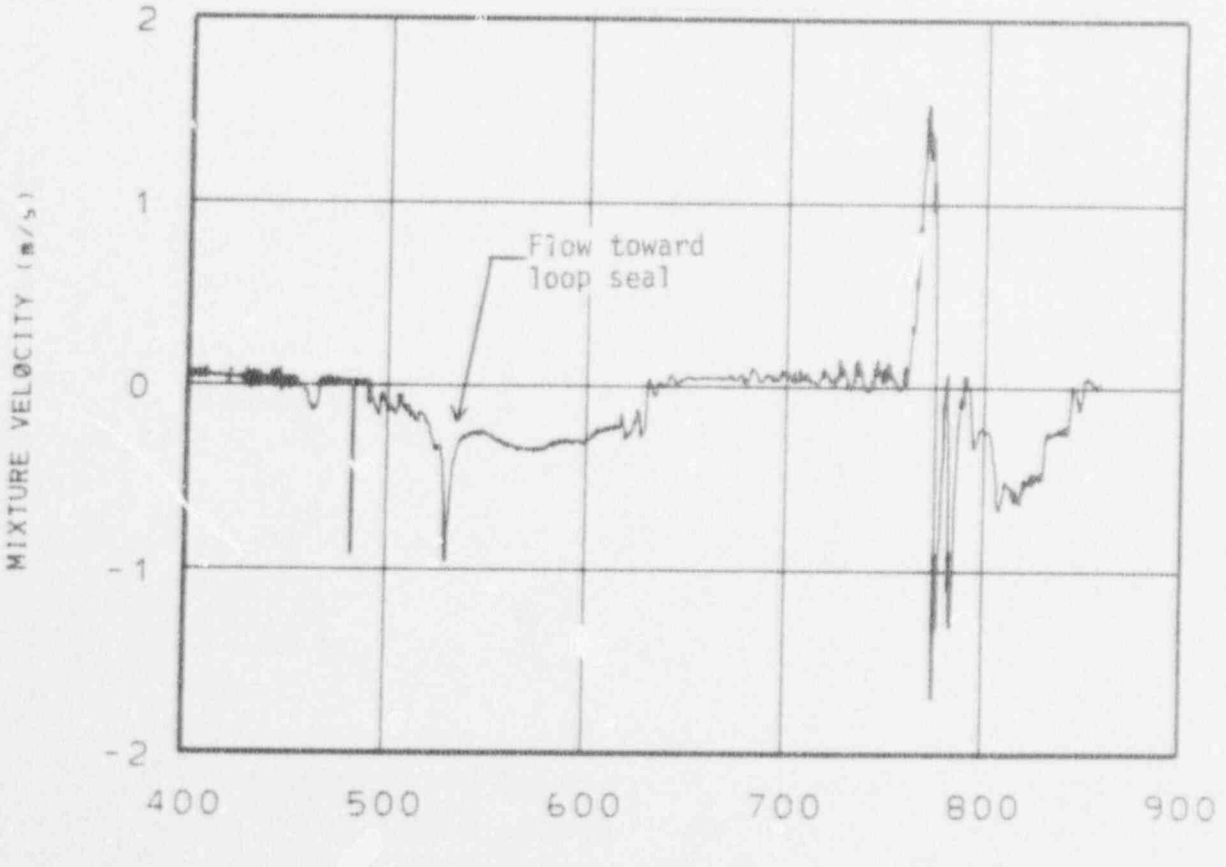

Figure 11. Intact loop mixture velocity, 400 s to 900 s (TRAC-P1A).

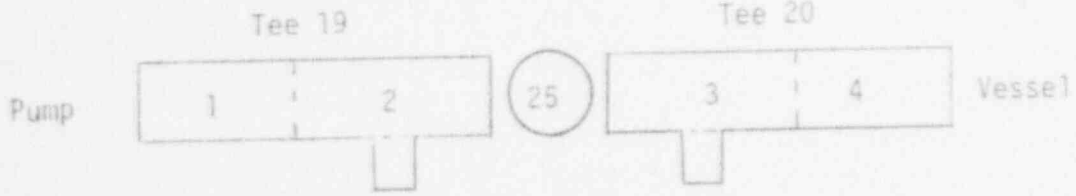

Curve identifiers correspond
to cell numbers

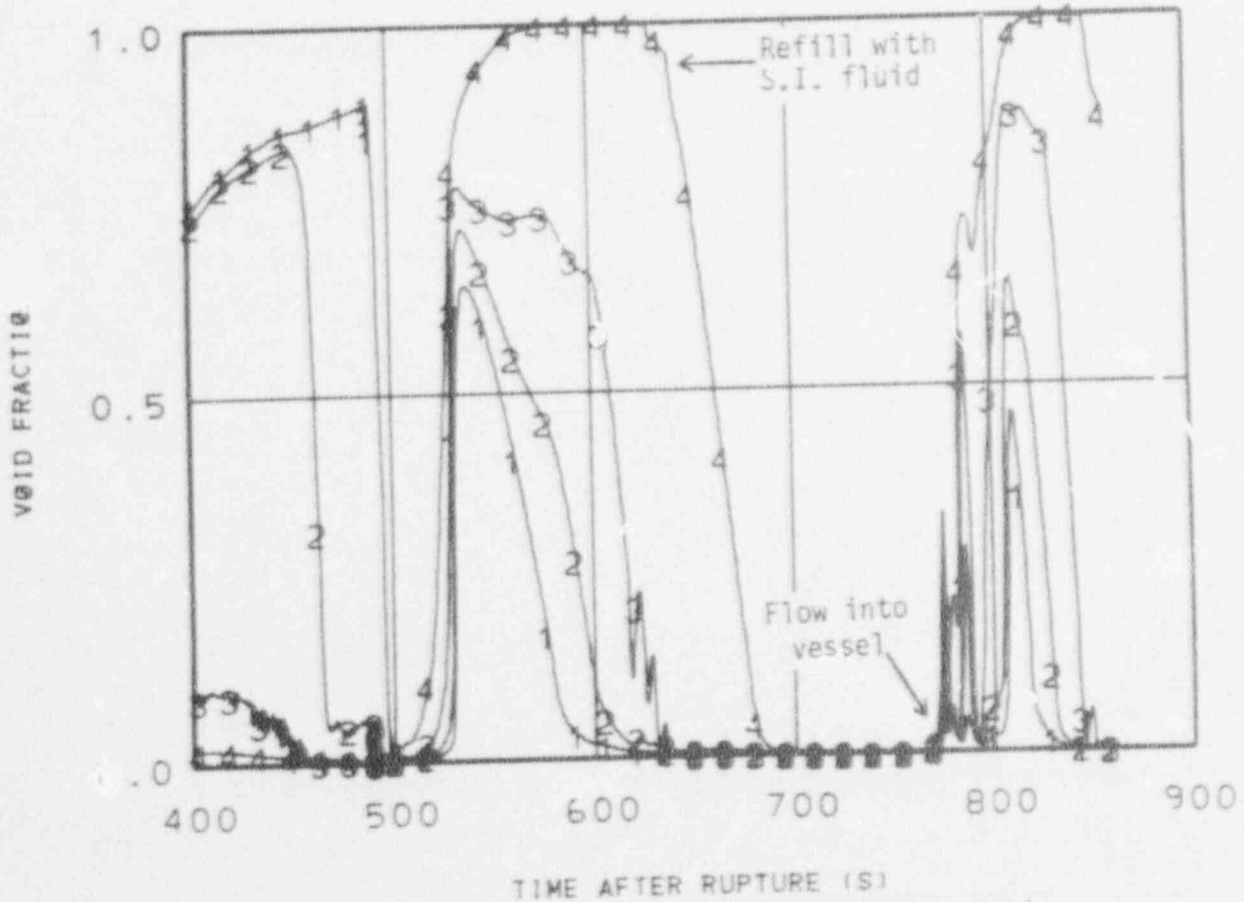

Figure 12. Void fraction intact cold leg (TRAC-P1A).

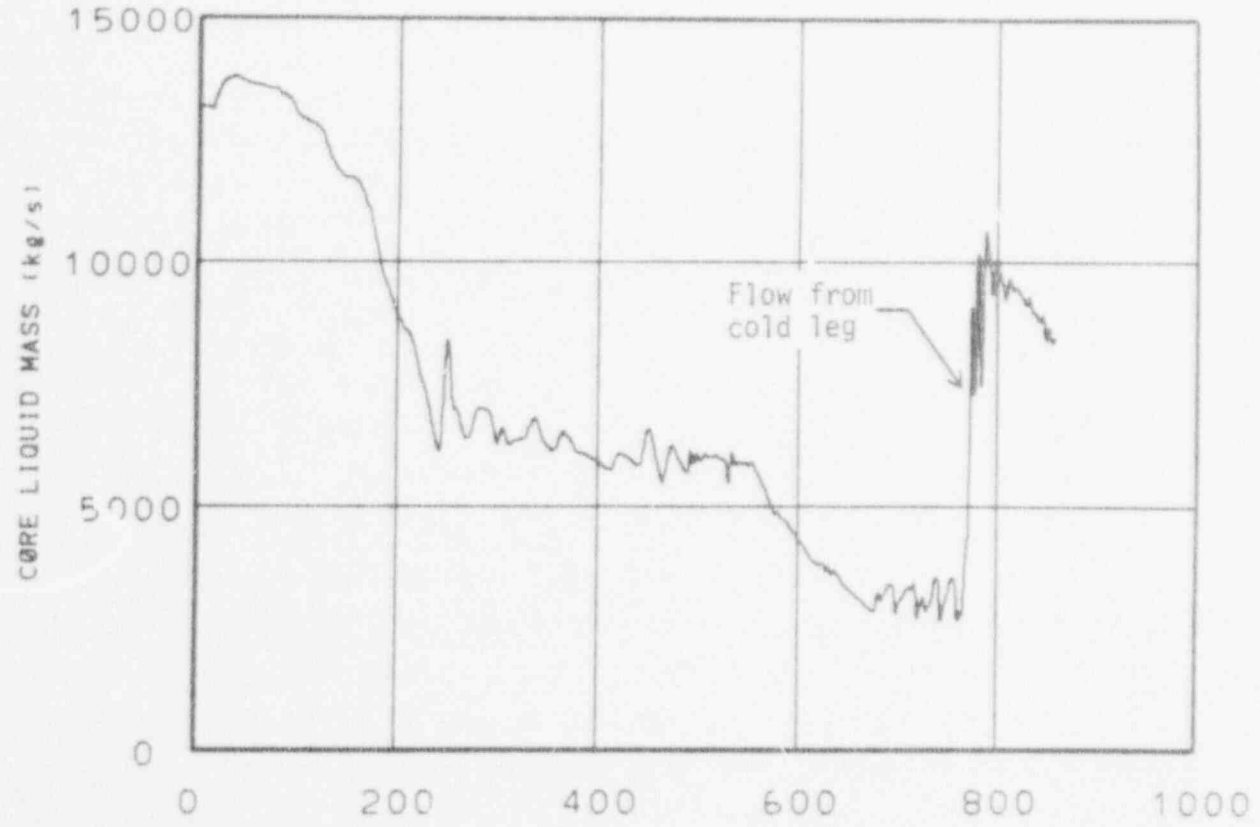

Figure 13. Core liquid mass (TRAC-P1A).

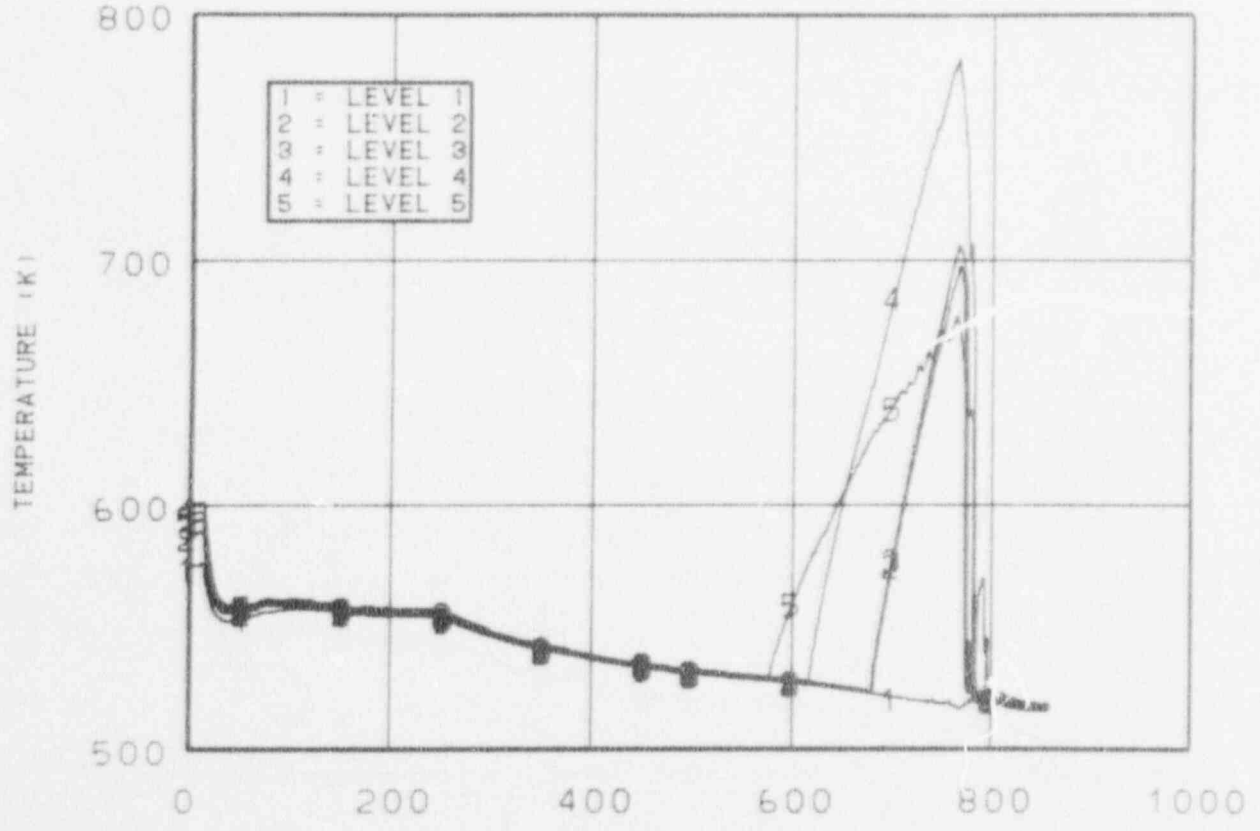

Figure 14. Rod 1 axial temperature profile (TRAC-P1A).

Comparisons of the TRAC-P1A small break calculation with TRAC-PD2 and RELAP4/MOD7 calculations and the trends of experimental data will be presented in Section 3.3.

3.2 0.10 m-diameter Cold Leg Break Using TRAC-PD2

This section will discuss the TRAC-PD2 calculation and compares the results with the TRAC-P1A calculation discussed in Section 3.1.

The small break transient began with the opening of the break at 0.0 s. The system pressure decreased to 12.82 MPa, the system low pressure scram setpoint, at 11.0 s with a reactor scram 3.40 s later at 14.4 s. The primary coolant pumps were tripped and the steam generator outlet valves were also closed at this time. The main feed and auxiliary feed flow was simulated the same as was discussed for the TRAC-P1A calculation in Section 3.1.

The upper plenum pressure, Figure 15, decreased to the saturation pressure of the upper plenum fluid at about 60 s. The pressure remained nearly constant during the next 230 s showing only a slight increase from vapor generation in the core. The primary system continued depressurizing at 290 s when the loop seal in the broken loop was cleared. Clearing the broken loop seal permitted vapor from the upper plenum to reach the break. Increased break volumetric flow resulted in the system depressurizing at a faster rate. The primary system depressurized to 4.13 MPa at 462 s and accumulator flow was initiated. The system pressure showed an increase in depressurization rate at 560 s when cold accumulator fluid entered the vessel causing condensation in the vessel and a decrease in pressure.

The steam generator secondary pressure, also shown in Figure 15, remained lower than the system pressure until 370 s. From 370 s to 440 s the two pressures were equal, after 440 s the primary pressure was lower as the primary system depressurized due to flow through the break. The auxiliary feedwater flow remained on during the TRAC-PD2 calculation, cooling the secondary. The mass conservation in the TRAC-PD2 calculation

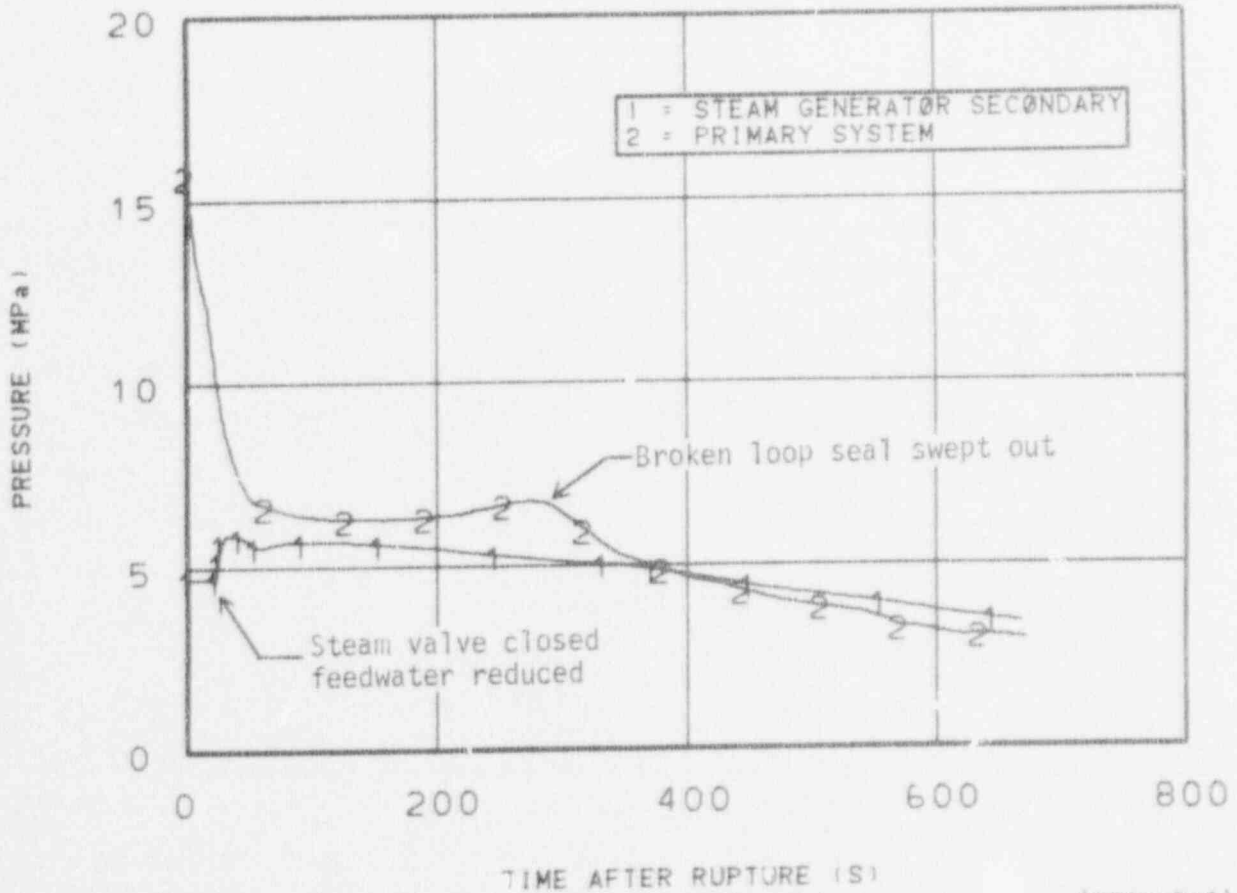

Figure 15. Upper plenum and steam generator secondary pressure (TRAC-PD2).

was very good. The rate of mass gain per unit time in the TRAC-PD2 steam generator secondaries matched the auxiliary feed flow with little error. With better mass conservation the water level in the steam generator did not recover by 400 s and the auxiliary feed system continued operating reducing the secondary temperature. Comparison of the TRAC-P1A with the TRAC-PD2 calculation at 650 s showed a secondary temperature of 532.5 K for TRAC-P1A and 515.5 K for TRAC-PD2. The reduced secondary temperature in the TRAC-PD2 calculation enhanced the primary system depressurization and shortened the time until accumulator initiation.

Steam generator secondary water level was controlled by the void fraction in the steam generator similar to previous TRAC calculations prior to the renoding of the steam generator. Future calculations should control the level on the downcomer indications since this is the method water level is maintained in an operating plant. Modeling the steam generator using the Steam Generator component and two Tees improved the performance of the steam generator. The new model allowed circulation within the steam generator during the transient eliminating severe temperature stratification which was observed in previous TRAC small break calculations. The model also allowed the preheating of feedwater during steady state calculations.

The break mass flow rate, shown in Figure 16, was initially 890 kg/s and decreased as the system pressure decreased to the hot leg saturation pressure of 6.6 MPa. The loop seal was swept out at 290 s which resulted in a high void mixture reaching the break reducing the break mass flow rate. Flow out of the vessel to the break reversed at 390 s causing a reduction in the break mass flow for about 10 s. The sharp decrease in break flow at 470 s was caused by stagnation of the flow between the vessel and the break. The stagnation occurred as a result of condensation in the vessel.

Flow in both loops decreased after the primary coolant pumps were tripped off at 14.3 s. At 150 s the flow in the broken cold leg between the vessel and break reversed, as shown in Figure 17. When the broken loop

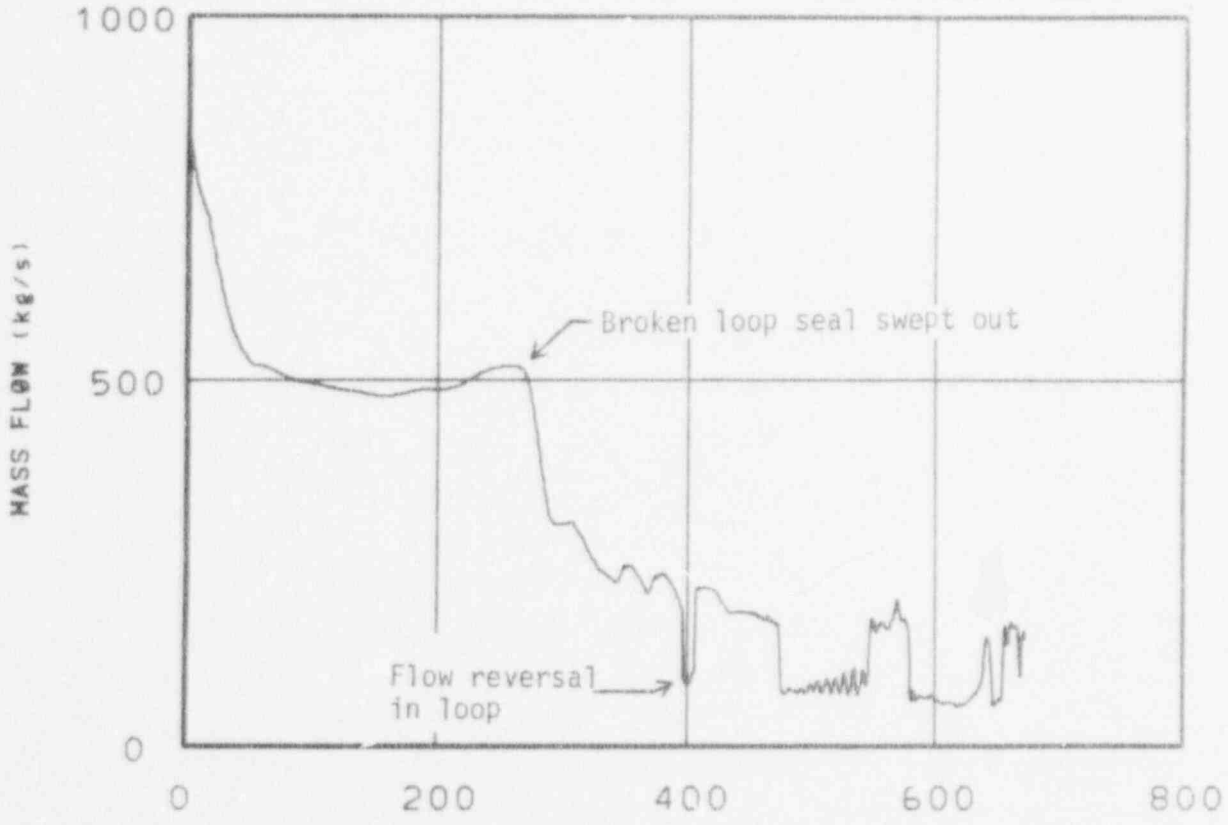

Figure 16. Break mass flow rate (TRAC-PD2).

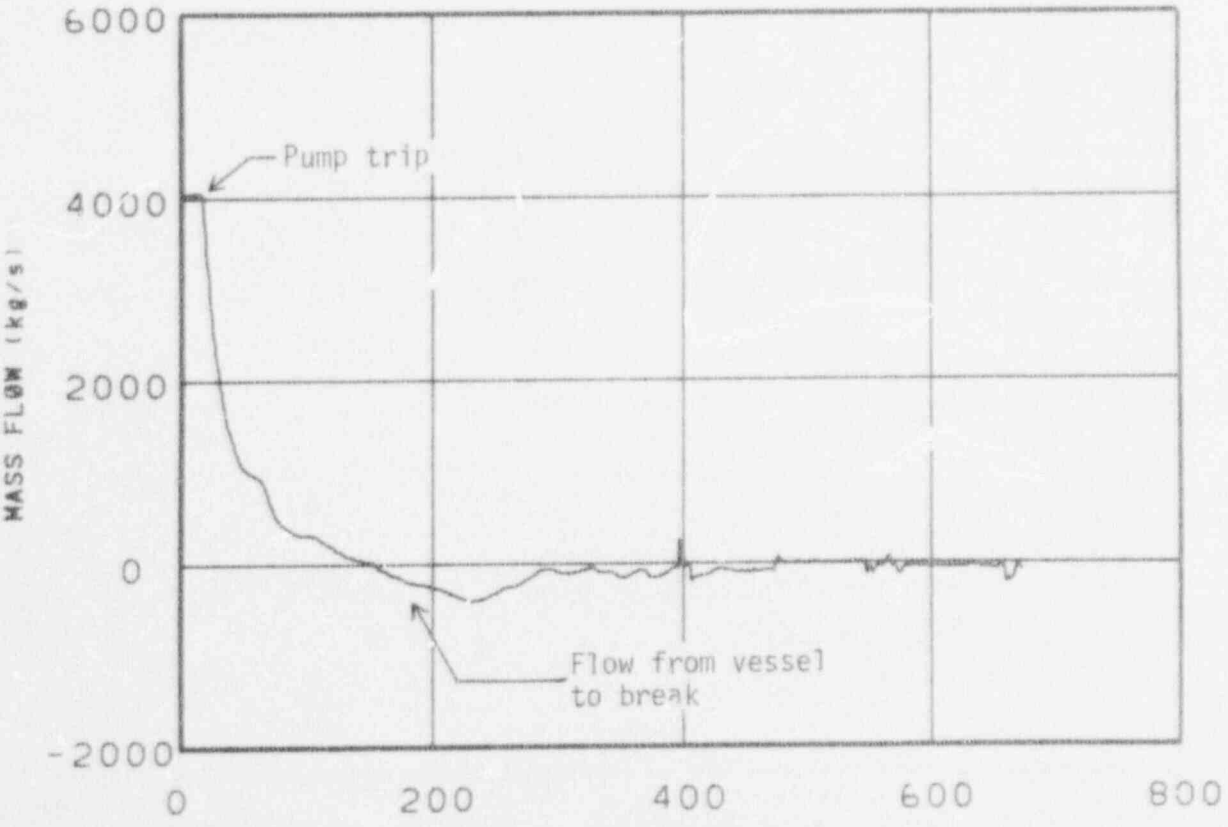

Figure 17. Broken cold leg mass flow (TRAC-PD2).

seal was swept out flow stagnated in the intact loop and a high void mixture circulated through the broken loop. Figure 18 shows the void fraction in the accumulator injection tee of the intact cold leg. The void fraction increased following the loss of the broken loop seal at 290 s. As the accumulator fluid entered the loop the void fraction was reduced. Prior to initiation of accumulator flow no liquid accumulated in the injection tee which differed from the TRAC-P1A calculated results. The intact loop pump seal was swept out at 570 s when pressure in the vessel was reduced by condensation allowing flow of the cold leg fluid to the vessel. In the TRAC-P1A calculation the intact loop seal remained liquid filled throughout the transient. The pump seal in the TRAC-P1A calculation may have remained filled due to the accumulation of the safety injection fluid in the seal. The increased mass in the loop seal in the TRAC-P1A calculation may have prohibited the seal from being swept out.

Rod cladding temperatures, shown in Figure 19, remained near saturation throughout the transient. Cooling was maintained by a two phase mixture flowing through the core. The peak clad temperatures were the normal operating temperatures at the start of the transient. No dryout of the cladding was calculated in the TRAC-PD2 calculation in contrast to the TRAC-P1A calculation. This was due in part to the earlier depressurization of the system and subsequent accumulator flow.

Comparisons of the TRAC-P1A and TRAC-PD2 calculations with other calculations and experimental data will be made in Section 3.3.

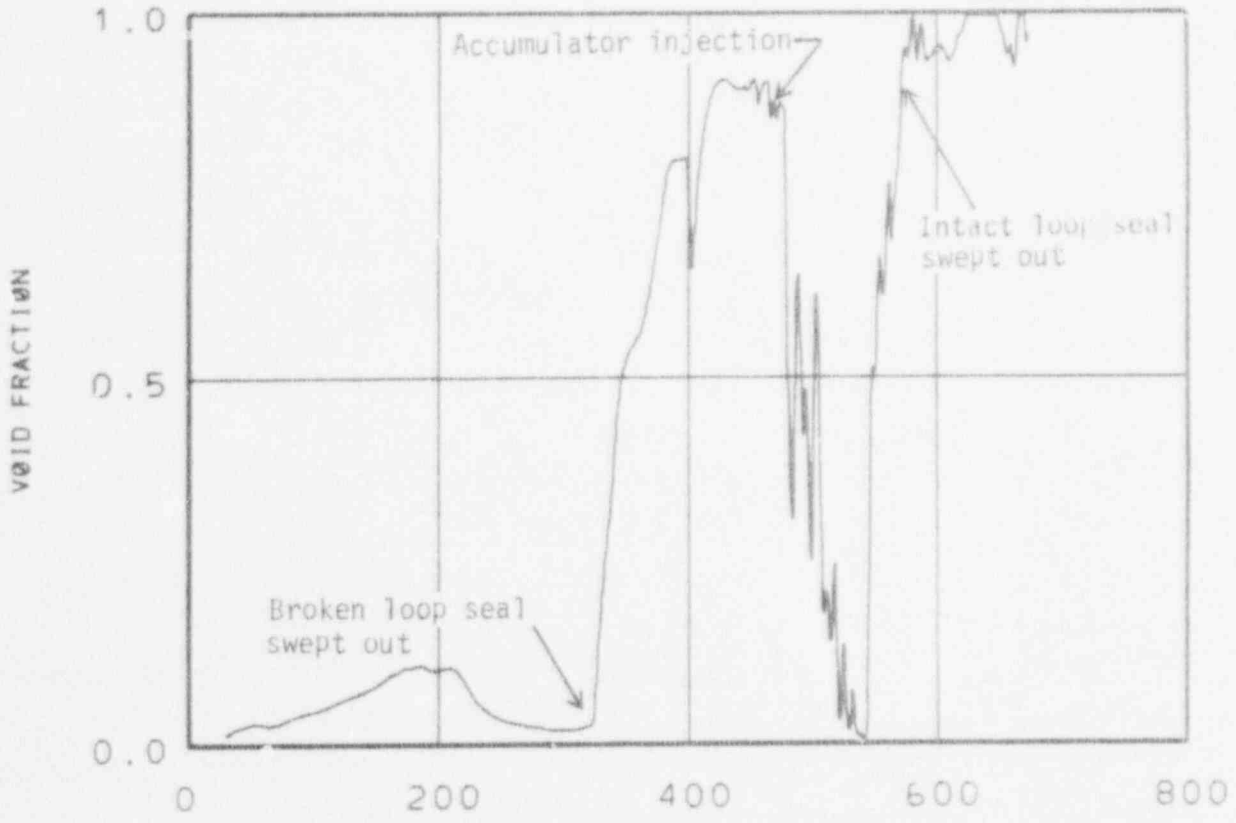

Figure 18. Vapor fraction intact cold leg (TRAC-PD?).

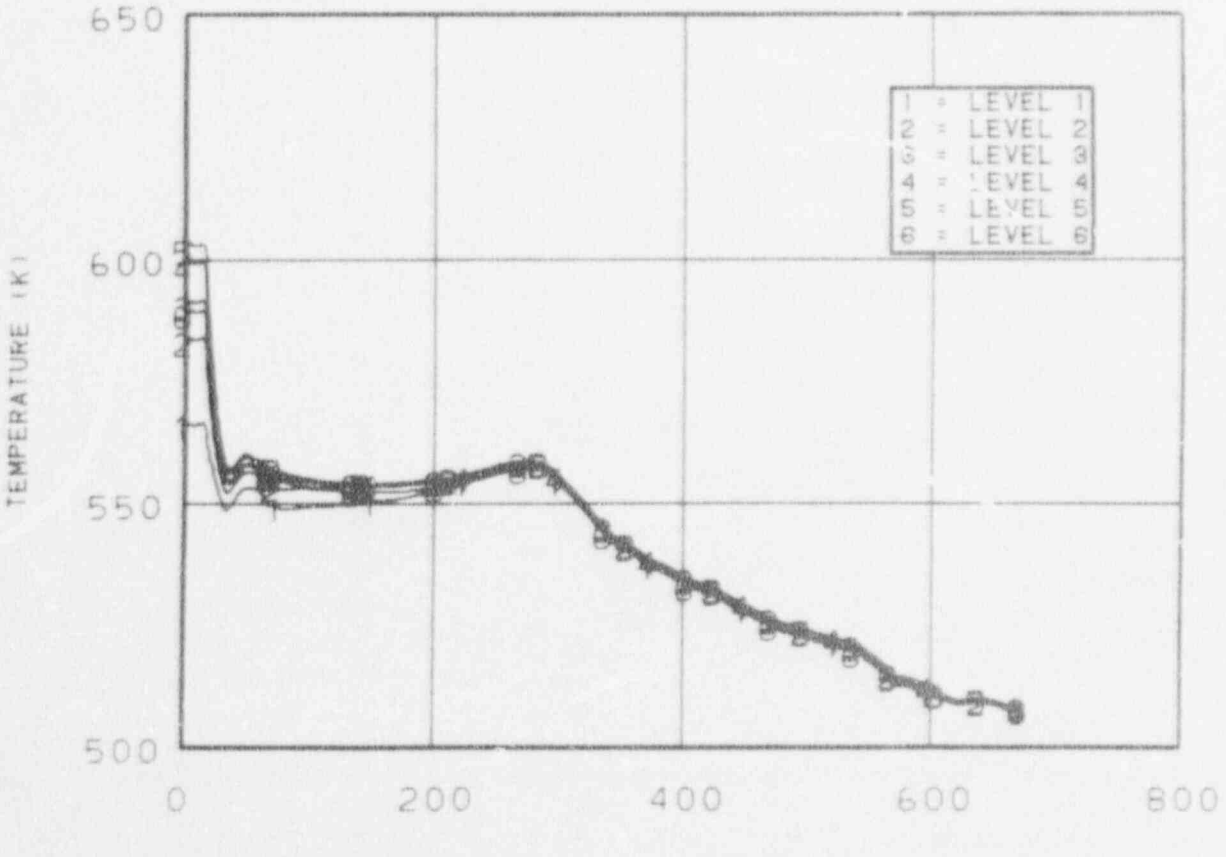

Figure 19. Rod 1 axial temperature profile (TRAC-PD2).

3.3 Comparisons of TRAC Small Break Calculations With Experimental Data and RELAP4/MOD7 Calculation

This section compares a few selected parameters from both TRAC calculations with the trends of experimental data and one RELAP4/MOD7 calculation. Semiscale Test S-SB-2[8] and LOFT experiment L3-1[9] were selected for comparison because both represented a 2.5% cold leg break. The RELAP4/MOD7[10] calculation simulated the same cold leg break transient as both of the TRAC calculations. The LOFT L3-1 experiment simulated reactor scram and primary coolant pump trip at 0.0 s in the transient. The Semiscale S-SB-2 test allowed pump trip and power decay to occur as the system pressure decreased. Both TRAC calculations and the RELAP4/MOD7 calculation tripped the coolant pumps and reduced the power upon low system pressure. The two experiments are compared with the two TRAC calculations and the RELAP4/MOD7 calculation in the following section. Even though there were minor differences in the experiments and calculations it was possible to make qualitative comparisons and observed the general trends of both the calculations and the data.

A comparison of the primary system pressure, Figure 20, shows that all three calculations and data are in good agreement early in the transient. The variation between the three calculations and the experimental data was approximately 1 MPa early in the transient. The variation was due to the differences in upper plenum fluid temperature which controls the saturation pressure. Under- or overpredicting the upper plenum temperature by 2 K results in a pressure difference of about 0.2 MPa. The TRAC-PD2 system pressure was the lowest after 400 s due to continued auxiliary feed flow which was terminated in the TRAC-P1A and RELAP4/MOD7 calculations. In both the Semiscale and LOFT experiments the auxiliary feed flow was not initiated until approximately 75 s but was continued troughout the remainder of the experiment.

A comparison of the steam generator secondary pressures, Figure 21, shows a wider dispersion of the data and calculations. The TRAC calculated pressures were lower than the LOFT value for several reasons. Secondary

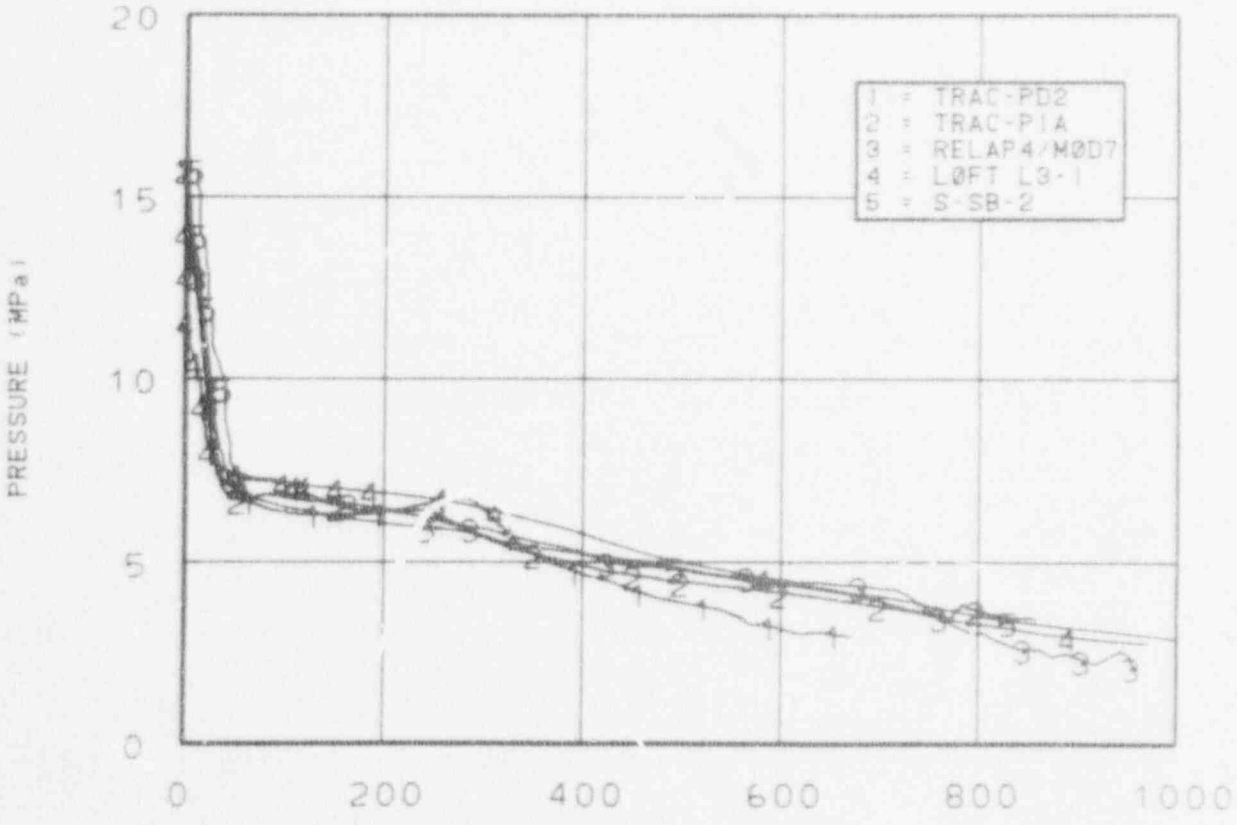

Figure 20. Upper plenum pressure comparison.

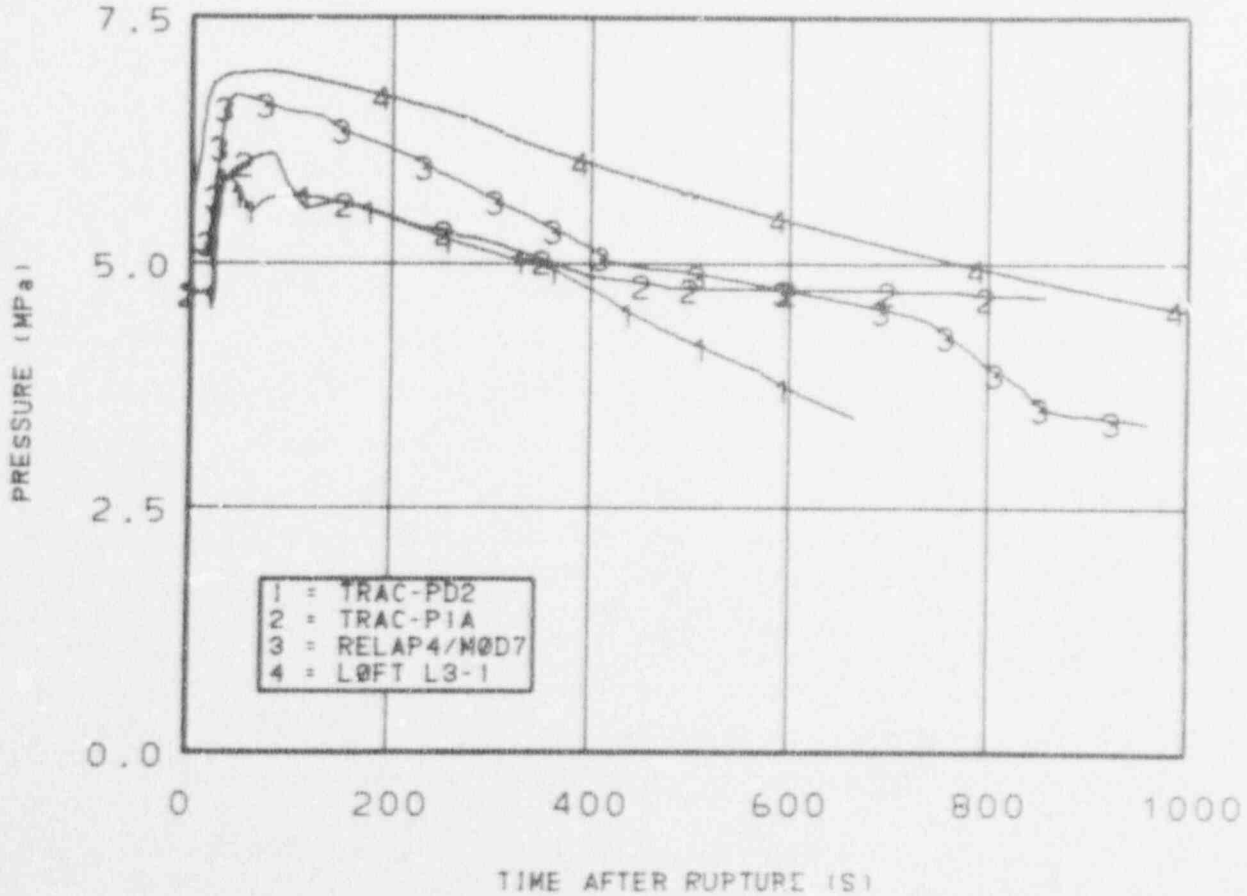

Figure 21. Steam generator secondary pressure comparison.

pressures in both TRAC calculations were lowered and feedwater flow rates increased to achieve an energy and a mass balance. The steam outlet valves in the LOFT experiment were manually closed at 0.0 s whereas the TRAC calculations the valves were closed at 19-20 s due to low primary system pressure. Auxiliary feedwater flow was not started until 75 to 80 s after the start of the transient in LOFT. The calculations simulated start of feedwater flow at approximately 30 s. Considering the difference in the TRAC calculation and the LOFT experiment it is reasonable to assume the pressure predicted would be closer if an actual simulation of the test had been conducted. All secondary pressures showed the same trends later in the calculation as the pressures decreased. The RELAP4/MOD7 calculation showed some cooling from the accumulator fluid between 740 and 860 s. All three calculations showed the same trends as the data early in the transient with some differences later in the transient due to auxiliary feedwater termination.

Break mass flow rate of the two TRAC and one RELAP4/MOD7 calculation are shown in Figure 22 along with the break mass flow rate for Semiscale Test S-SB-2. Each calculation showed an initial flow between 1000 and 900 kg/s which quickly decreased to about 500 kg/s. The two TRAC calculations indicated the loop seal was swept out at 270 to 290 s. The break flow became two phase after the loop seal was swept out at 490 s in the RELAP4/MOD7 calculation. With the decrease in density associated with steam reaching the break, the calculated break mass flow rates of all calculations decreased. The Semiscale test data showed similar trends. The break flow decreased as the system pressure reached saturation and remained nearly constant until the loop seal was swept out at about 200 s. During the RELAP4/MOD7 calculation the break mass flow increased after initiation of the accumulator flow due to the homogeneous mixing of subcooled liquid with the steam in the cold leg.

Rod cladding temperatures in each calculation remained near the saturation temperature early in the transient as shown in Figure 23. The trends of the experimental data compare well with the TRAC and RELAP4/MOD7

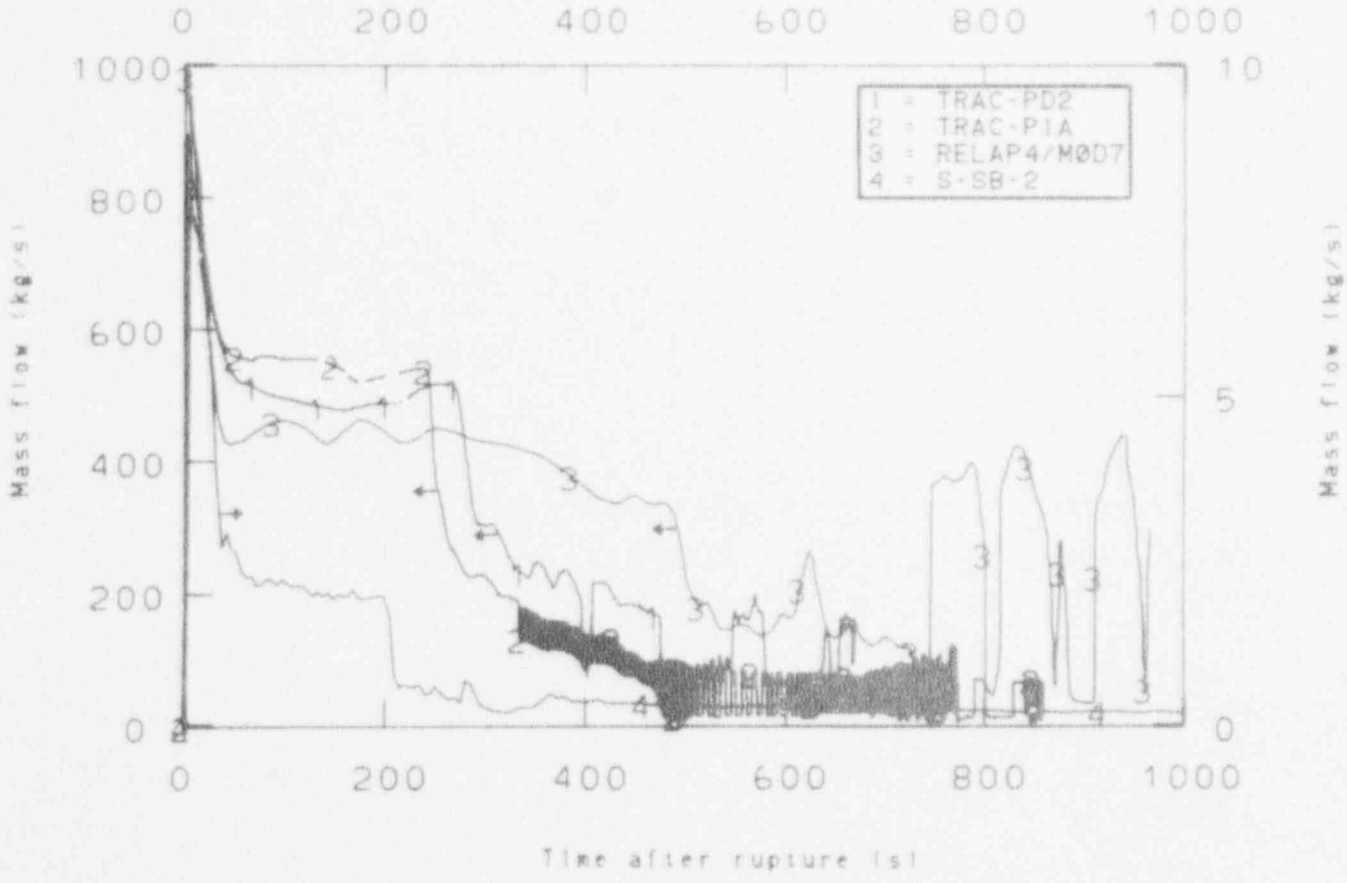

Figure 22. Calculated break mass flow comparison.

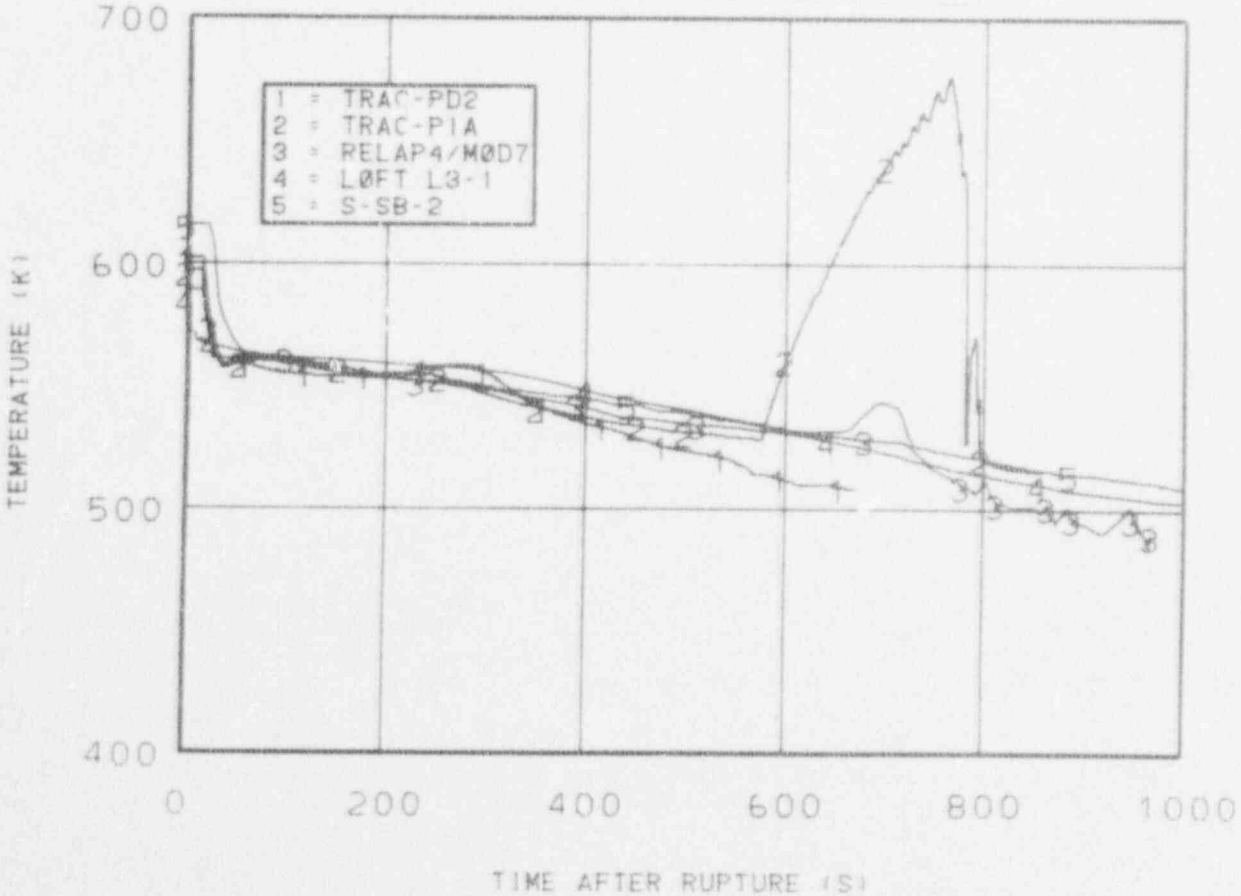

Figure 23. Rod cladding temperature comparison, upper elevation.

calculated results. The TRAC-P1A calculation indicated a cladding dryout and an increase in temperature at 590 s which was not calculated by TRAC-PD2 or RELAP4/MOD7 and was not observed experimentally. Both experimental data and calculated rod cladding temperatures were near 500 K at the termination of the transient.

3.4 Single Steam Generator Tube Rupture Calculation

The steam generator tube rupture calculation simulated the 200% offset break of a single steam generator tube at the tube sheet. The ruptured tube was the only path of primary coolant loss modeled for the transient. The steam generator tube rupture occurred at 0.0 s in the transient. Decreasing system pressure resulted in a primary pump trip and a reactor scram. The charging and safety injection system was activated at 100 s upon low pressurizer pressure. Feedwater flow to the ruptured secondary was reduced at 30 s by an amount equal to the primary to secondary leakage rate. The reduced feedwater flow modeled the action of an automatic feedwater flow controller in a typical plant. The calculation was terminated at 600 s because the safety injection flow exceeded the leakage to the steam generator secondary and continuing the calculation would not yield significant new information.

The upper plenum pressure shown in Figure 24 decreased to 12.82 MPa at 97 s which resulted in a reactor scram, primary coolant pump trip, and isolation of the steam generator steam line at 100 s. The main feedwater was ramped off from 100 to 114 s and auxiliary feed flow was started at 115 s. The rate of depressurization increased after the scram as a result of the decreased heat addition to the fluid passing through the core. As the transient progressed, the system depressurization slowed with the steam generator secondary pressure and primary system pressure approaching each other.

The secondary pressure in the ruptured steam generator, shown in Figure 25, showed a slight increase at the start of the transient, but remained near its normal value for the first 100 s of the transient. The

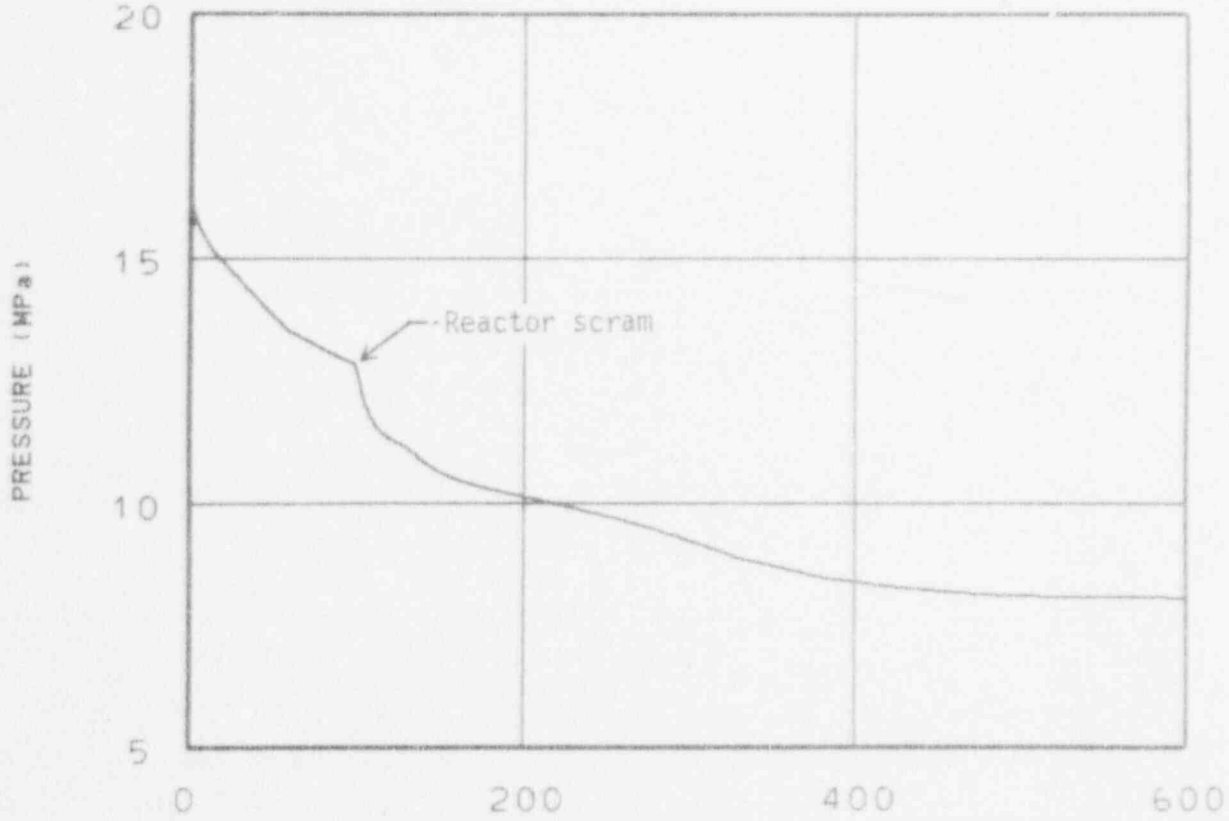

Figure 24. Upper plenum pressure, steam tube rupture.

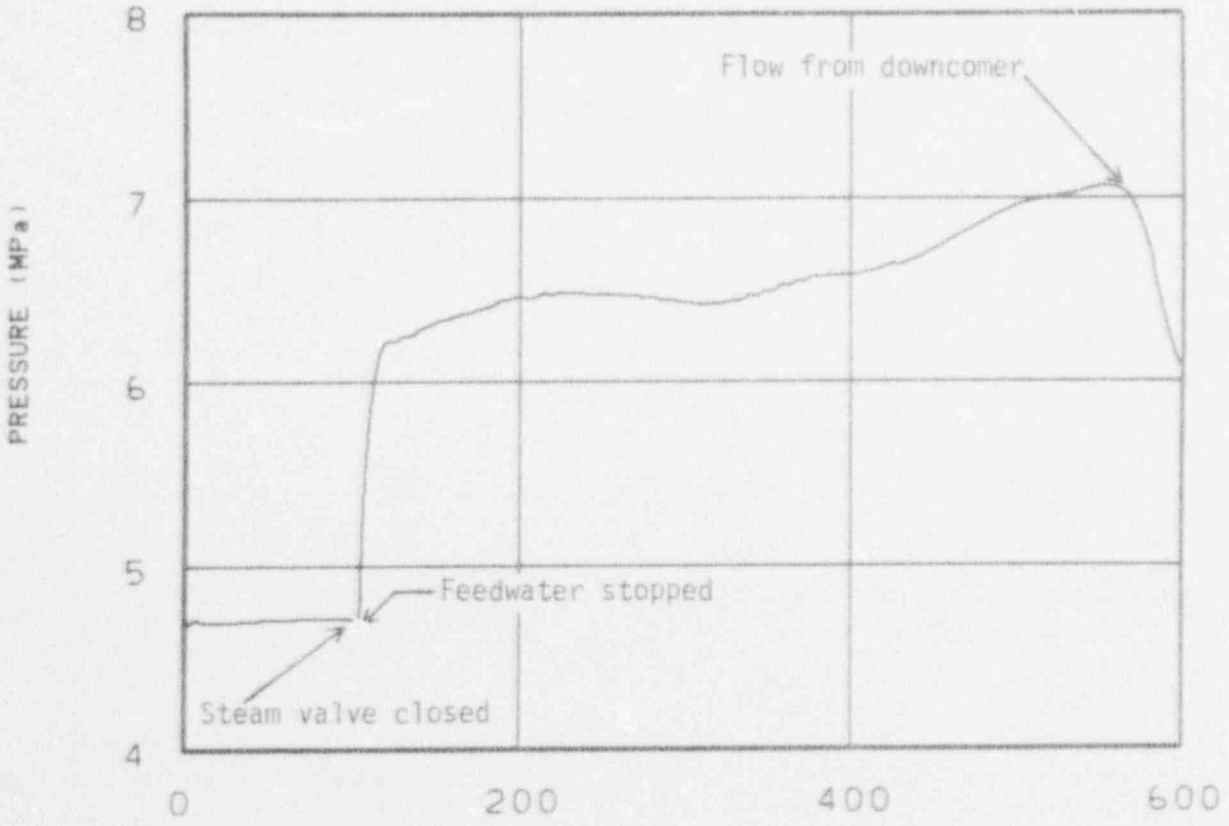

Figure 25. Ruptured steam generator secondary pressure.

pressure dropped slightly due to continued feed flow after the scram, at 100 s, and the steam outlet valve was shut. Secondary pressure then increased sharply as the feed flow was reduced, but did not reach the safety valve setpoint. Auxiliary feedwater flow was terminated at 426 s and the pressure increased until 570 s. At 540 s the flow in the steam generator downcomer reversed, as shown in Figure 26, and cool fluid was forced into the upper parts of the steam generator reducing the pressure. The secondary pressure would be expected to once again increase as the downcomer temperature reached equilibrium with the rest of the steam generator.

Flow through the ruptured tube, shown in Figure 27, was slightly over 100 kg/s initially. Flow decreased with primary system pressure until the steam valve was closed and feedwater flow was terminated at about 100 s. The increased secondary side pressure, after the steam valve closure, raised the downstream pressure resulting in an increase in the flow through the ruptured tube. The flow then decreased with the primary system pressure until the flow reversal in the steam generator downcomer reduced the secondary pressure. As the downcomer temperature reached equilibrium with the rest of the steam generator the secondary pressure was expected to increase reducing the flow from primary to secondary. The flow in the ruptured steam generator tube, had the calculation continued, would approach zero as the steam generator filled and the system pressure approached the secondary pressure.

Flow through the primary system decreased after the pump trip and a steady natural circulation was maintained as shown in Figure 28. Flow in the primary coolant system removed the heat from the core and the intact loop steam generator was adequate to remove the decay heat. The core remained full of fluid throughout the transient as shown in Figure 29. The decrease in liquid volume in the core was insignificant and was recovering when the transient was terminated. Continuing the calculation beyond 600 s would have shown the pressurizer filling with liquid as the steam generator secondary and primary system differential pressure decreased and reached equilibrium.

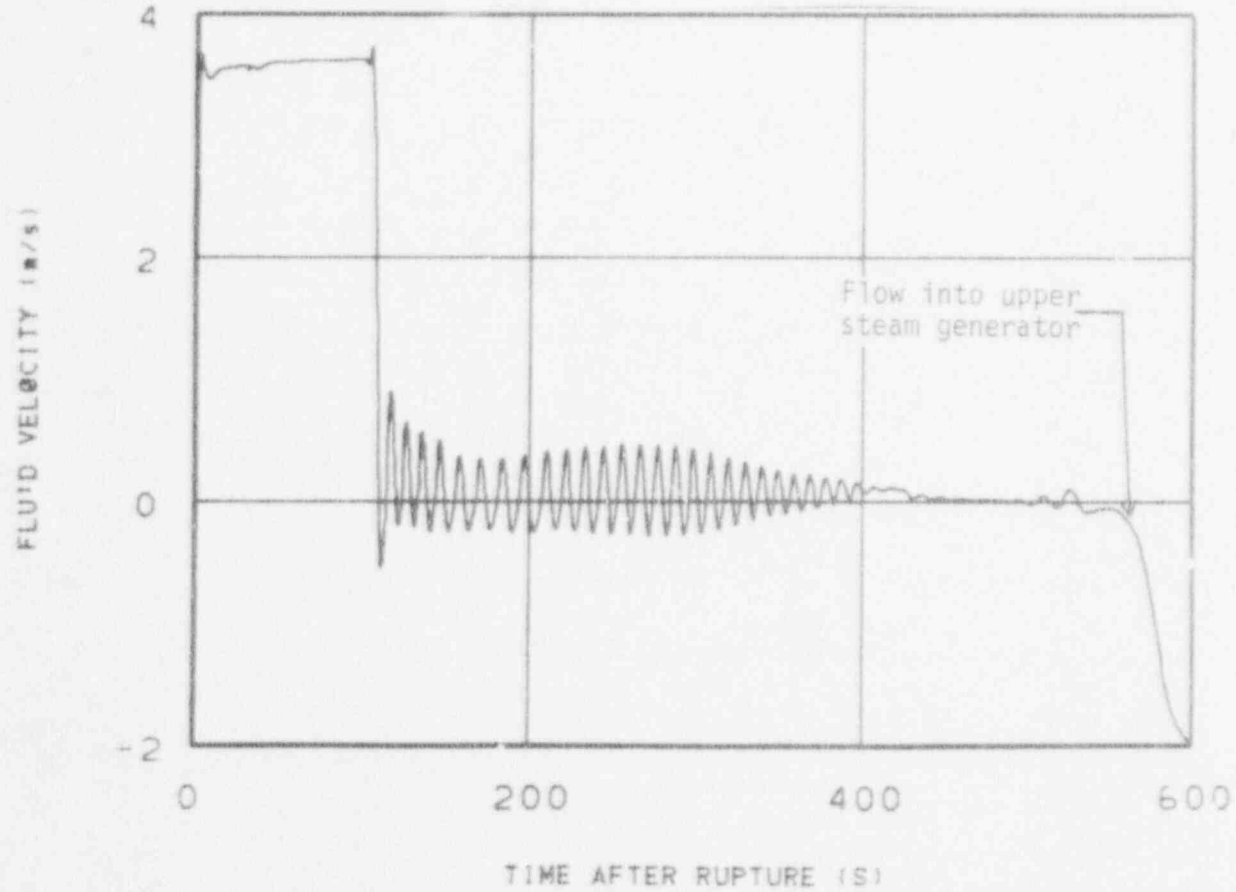

Figure 26. Steam generator downcomer fluid velocity, steam tube rupture.

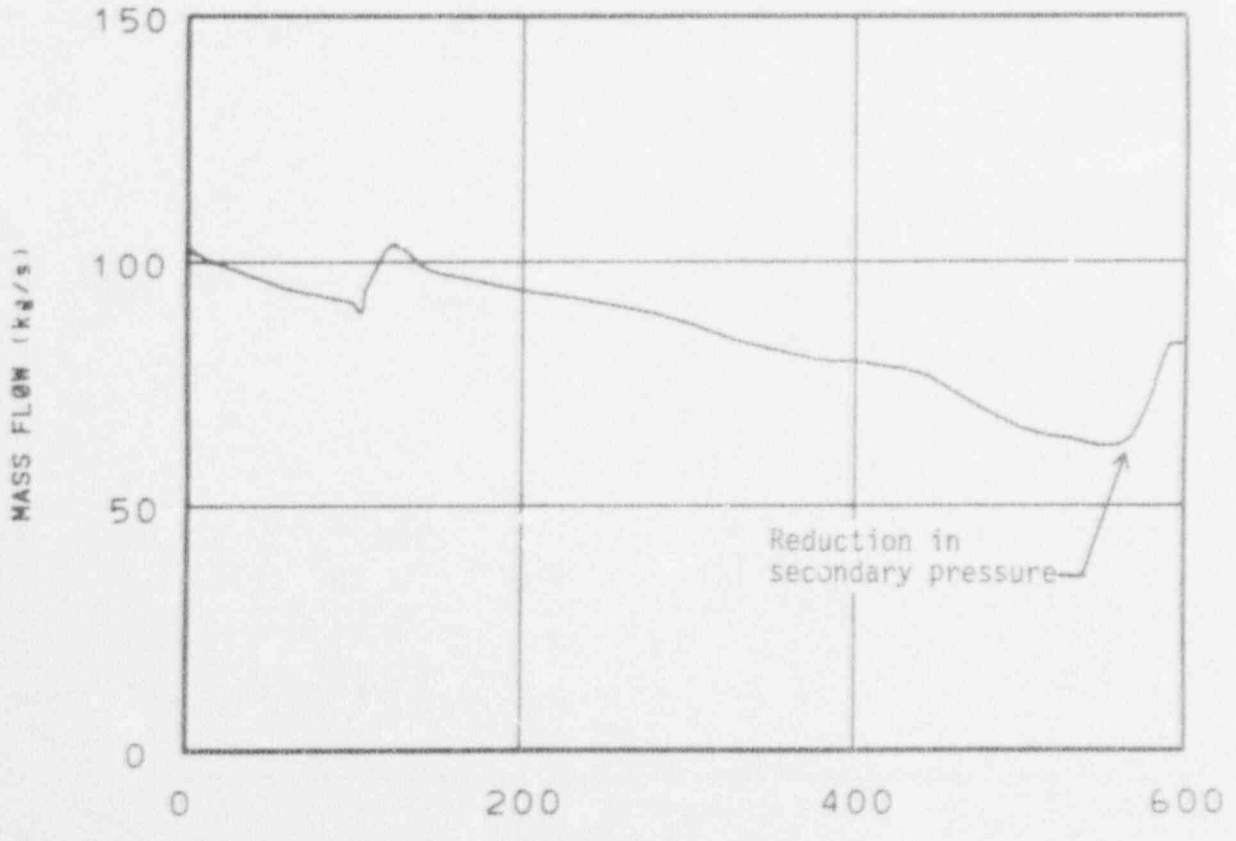

Figure 27. Mass flow through rupture tube, steam tube rupture.

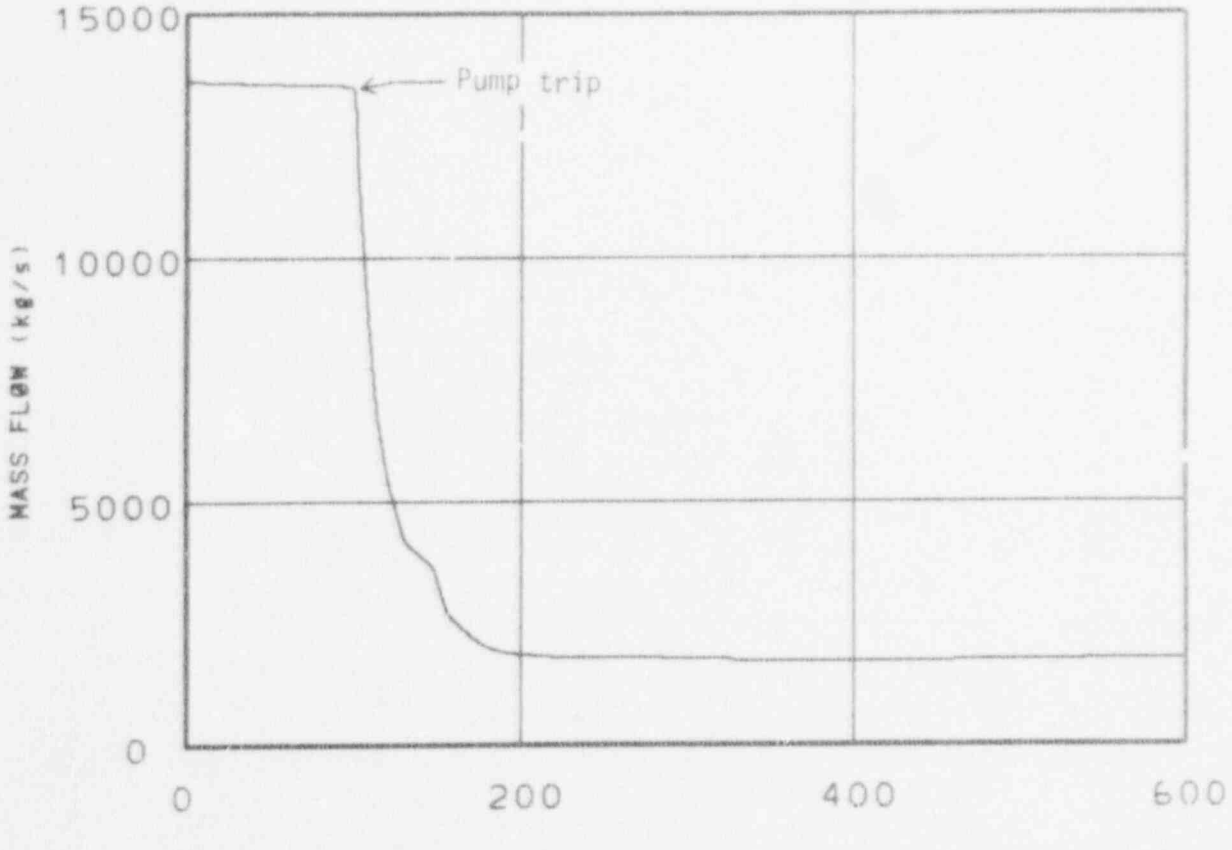

Figure 28. Intact cold leg mass flow, steam tube rupture.

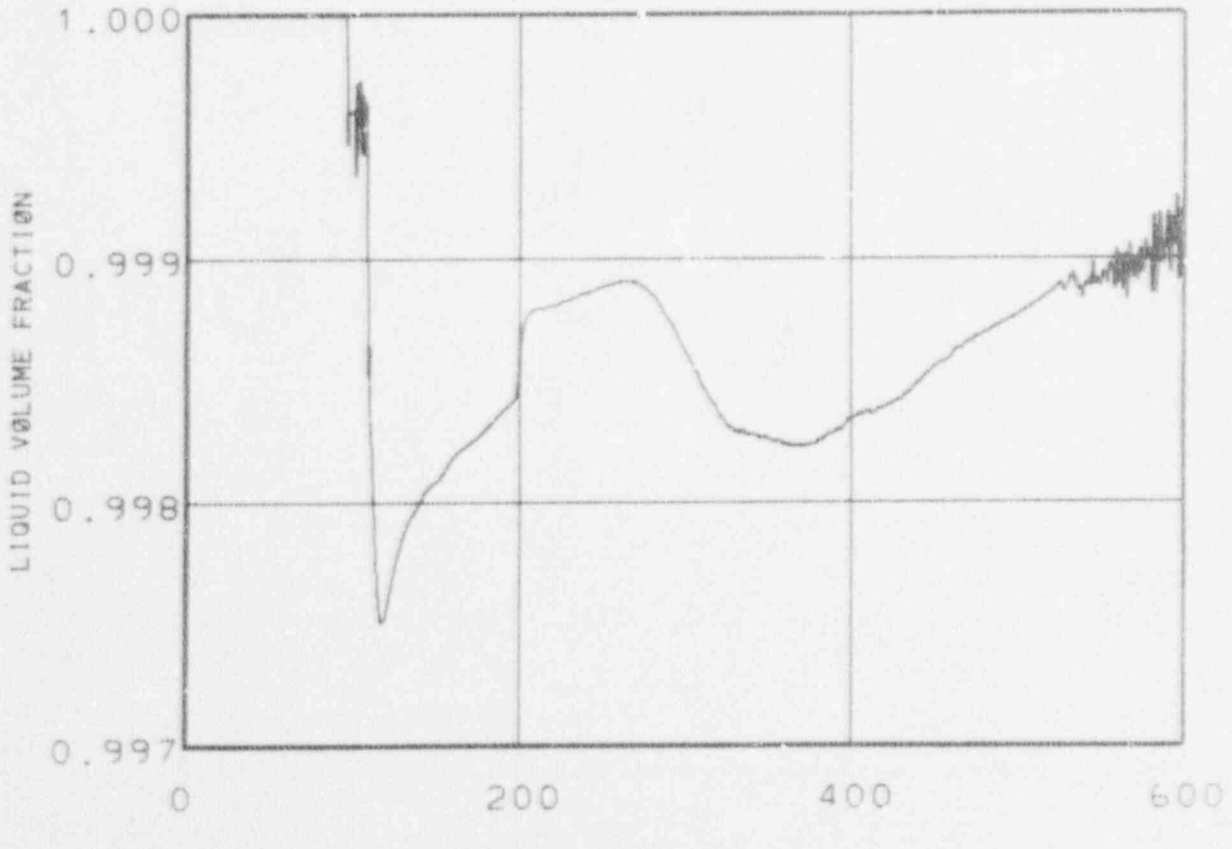

Figure 29. Core liquid volume fraction, steam tube rupture.

The results of the TRAC-PD2 steam tube rupture calculation compared qualitatively with events that occurred at utilities which have experienced tube ruptures [11]

4. CONCLUSIONS AND RECOMMENDATIONS

1. *TRAC-P1A and TRAC-PD2 were capable of calculating the general system hydraulics and core thermal response during a small cold leg break and steam generator tube rupture transients.*

2. *The steam generator modeling used in the calculations improved the performance of the steam generator by elimination of excessive temperature stratification.* The model also provides a method of representing recirculation and feedwater preheating.

3. *Rod cladding temperature increases were calculated by TRAC-P1A which were not observed experimentally or calculated by TRAC-PD2 and RELAP4/MOD7.* The increased cladding temperature may be due to the calculational mass error occurring in the TRAC-P1A calcualtion.

4. *TRAC-PD2 showed a better capability to conserve mass during the small cold leg break calculation than TRAC-P1A did.* Mass conservation is especially important in the steam tube rupture sequence when the secondary side fills with primary fluid.

5. *The TRAC-PD2 small break calculation showed trends similar to the available data.* The calculated rod cladding temperatures compared well with the experimental results of both LOFT L3-1[9] and Semiscale S-SB-2[10] staying near saturation temperature throughout the transient.

REFERENCES

1. TRAC-P1A, An Advanced Best-Estimate Computer Program for PWR LOCA Analysis, LA-7777-MS, May 1979.

2. R. J. Pryor, Letter to P. North, June 30, 1980.

3. G. W. Johnson et al., A Comparison of "Best Estimate" and "Evaluation Model" LOCA Calculations; The BE/EM Study, EG&G Idaho, Inc., Report PG-R-76-009, December 1976.

4. Zion Station Final Safety Analysis Report, Docket No. 50-295 (with ammendments).

5. J. Sicilian, TRAC Newsletter, Number 1, Los Alamos Scientific Laboratory, July 1979.

6. J. C. Vigil et al., TRAC-P1A Developmental Assessment, LA-8056-MS, October 1979.

7. P. D. Wheatley, M. A. Bolander, TRAC-P1A Calculations for a 200%, 0.25 m-diameter and 0.10 m-diameter Cold Leg Break in a Pressurized Water Reactor, EG&G Idaho Inc. EGG-CAAP-5190, June 1980.

8. D. H. Miyasaki, Experimental Data Report for Semiscale Mod-3 Small Break Test Series (Test S-SB-2 and S-SB-2A), NUREG/CR-1459, June 1980.

9. P. D. Bayless et al., Experimental Data Report for LOFT Nuclear Small Break Experiment L3-1, NUREG/CR-1145, January 1980.

10. C. A. Dobbe, RELAP4/MOD7 Small Break Sensitivity Studies (to be published).

11. Nuclear Power Experience, Vol. PWR-2, Section V, Reactor Coolant Systems, D. Steam Generators, Articles 60, 236, 246.

APPENDIX A

CODE INPUT LISTING

The following contains the input and changes for the TRAC-P1A 0.10 m-diameter cold leg break, TRAC-PD2 0.10 m-diameter cold leg break, and the TRAC-PD2 steam tube rupture calculation.